Proposal to JLab PAC 53 Double Deeply Virtual Compton Scattering with SoLIDμ spectrometer

Alexandre Camsonne
Jefferson Laboratory Hall A
June 17th 2025
Hall A/C collaboration meeting

U.S. DEPARTMENT OF ENERGY | Office of Science
Jefferson Lab
Thomas Jefferson National Accelerator Facility
JSA

Proposal to PAC53 PR12-25-010

Proposal to JLab PAC 53

Double Deeply Virtual Compton Scattering with SoLIDμ spectrometer

Xinzhan Bai*, Alexandre Camsonne*†, Silviu Covrig Dusa, Kondo Gnanvo, Dave Mack, Michael McCaughan, and Richard Tyson

Thomas Jefferson National Accelerator Facility, Newport News, VA, USA

Juan-Sebastian Alvarado*, Raphaël Dupré, Adam Hobart, Dominique Marchand, Carlos Muñoz Camacho, Silvia Niccolai, and Eric Voutier*

Université Paris-Saclay, CNRS/IN2P3/IJCLab, Orsay, France

Haiyan Gao, Yining Liu, Bo Yu, Yi Yu, Zhiwen Zhao*, and Jingyi Zhou

Duke University, Durham, NC, USA

Keagan Bell, Debaditya Biswas, Marie Boër*, Gyang Chung, Mahmoud Gomina, Arna Ma, and Kemal Tezgin

Virginia Tech, Blacksburg, VA, USA

Garth Huber, Nathan Heinrich, Muhammad Junaid, Vijay Kumar, and Alicia Postuma

University of Regina, Regina, SK, Canada

Ronald Gilman

Rutgers University, Piscataway, NJ, USA

Nilanga Linayage, Huong Thi Nguyen, and Asar Ahmed

University of Virginia, Charlottesville, VA, USA

Yi Wang, Junhuai Xu, Zhihong Ye, Haojie Zhang, and Yaopeng Zhang

Tsinghua University, Beijing, China

Evaristo Cisbani

Istituto Superiore di Sanità, Roma, Italia

Guido Maria Urcioli

INFN, Sezione di Roma1, Roma, Italia

Vincenzo Bellini and Concetta Maria Sutera

Università di Catania, Catania, Italia

Anthony W. Thomas

ARC Special Research Centre for the Subatomic Structure of Matter (CSSM), University of Adelaïde, Adelaïde, Australia

Pierre Chatagnon[1], Maxime Defurne[1], Víctor Martínez-Fernández[1,2], Hervé Moutarde[1], and Franck Sabatié[1]

[1] *IRFU, CEA, Université Paris-Saclay, Gif-sur-Yvette, France*

[2] *Center for Frontiers in Nuclear Science, Stony Brook University, Stony Brook, NY, USA*

Malek Mazouz and Wassim Hamdi

Faculté des Sciences de Monastir, Département de Physique, Monastir, Tunisia

Whitney Armstrong, Sylvester Joosten, and Zein-Eddine Meziani

Argonne National Laboratory, Physics Division, Argonne, IL, USA

Thomas Hemmick

Stony Brook University, Stony Brook, NY, USA

Bernard Pire

Centre de Physique Théorique, CNRS, École polytechnique, I.P. Paris, Palaiseau, France

Pawel Sznajder and Jakub Wagner

National Centre for Nuclear Research, NCBJ, Warsaw, Poland

Johan A. Colorado-Caicedo

Centro de Investigacion y de Estudios Avanzados del Instituto Politecnico Nacional,San Pedro Zacatenco, Mexico City, Mexico

Sudip Bhattarai

Idaho State University,Pocatello, ID, USA

Nikos Sparveris, Hamza Atac, Suman Shrestha, and Mazmus. Ifat

Temple University, Philadelphia, PA, USA

Mostafa Elaasar

Southern University at New Orleans,New Orleans, LA,USA

Darko Androić

University of Zagreb, Faculty of Science, Zagreb, Croatia

Eric Fuchey

College of William & Mary, Williamsburg, Virginia, USA

Hem Bhatt

Mississippi State University, Mississippi State, MS, USA

Pawel Nadel-Turonski

University of South Carolina, Columbia, SC, USA

Xiaqing Li, Tianbo Liu, and Weizhi Xiong

Shandong University, Qingdao, Shandong, China

*: Co-spokesperson, †: Contact-spokesperson (camsonne@jlab.org)

And SoLID collaboration

Spokesperson : Juan-Sebastian Alverado, Alexandre Camsonne, Marie Boer, Eric Voutier, Xinzhan Bai, Zhiwen Zhao

Overview

- General Parton Distributions
- Double Deeply Virtual Scattering
- SoLIDμ setup
- Muon detector
- Simulation study
- Physics projections
- Beam time request
- Conclusion

Electron scattering

Elastic scattering
gives Form Factors : spatial
distribution of quarks

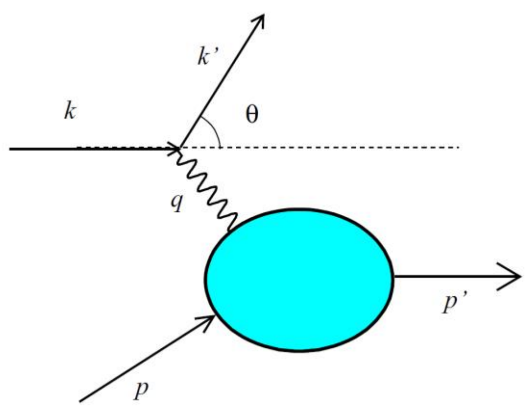

Deep Inelastic Scattering
gives access to partons distributionquark
content of nucleons

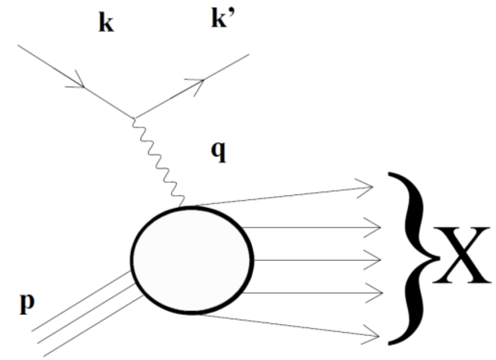

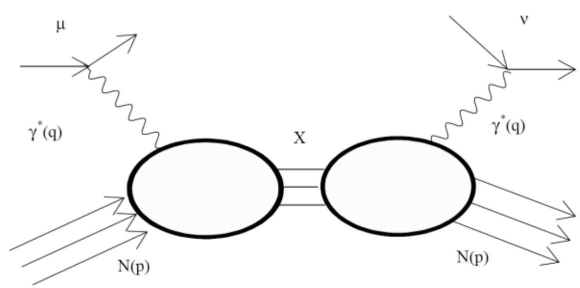

Spin crisis :
spin of nucleon is not simple sum of spin of quarks
Quarks are a more dynamic system inside of the nucleon so more information about quarks inside of nucleon is needed

Generalized Parton Distributions

Generalized Parton Distributions are a generalization of Form Factor and Partons Distributions

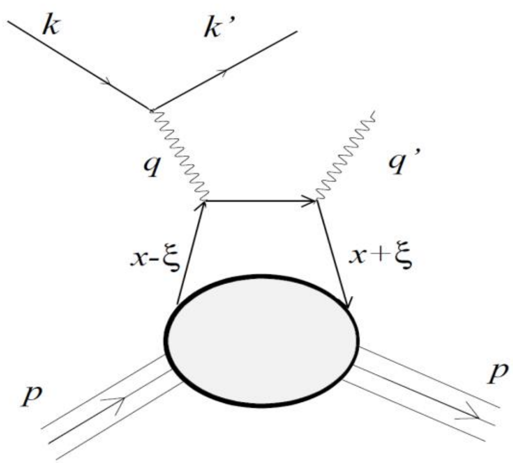

$$P = \frac{p+p'}{2} \qquad q_M = \frac{q+q'}{2}$$

$$\Delta = p - p'$$
$$t = (p-p')^2 = \Delta^2$$
$$s = (p+q)^2 = W^2$$
$$\bar{M}^2 = P^2 = M^2 + t/4$$

$$p^\mu = \frac{\Lambda}{\sqrt{2}}(1,0,0,1) \quad n^\mu = \frac{1}{\Lambda\sqrt{2}}(1,0,0,-1)$$

$$\xi = \frac{\Delta \cdot q_M}{P \cdot q_M}$$

Properties of GPDs

- Forward limit ($\xi = 0$)

$$
\begin{aligned}
H^q(x,\xi=0,t=0) &= q(x)\,,\\
\widetilde{H}^q(x,\xi=0,t=0) &= \Delta q(x)\,,
\end{aligned}
$$

- Integration gives back form factors

$$
\begin{aligned}
\int_{-1}^{+1} dx H^q(x,\xi,t) &= F_1^q(t)\,, \quad \int_{-1}^{+1} dx E^q(x,\xi,t) = F_2^q(t)\,,\\
\int_{-1}^{+1} dx \widetilde{H}^q(x,\xi,t) &= G_A^q(t)\,, \quad \int_{-1}^{+1} dx \widetilde{E}^q(x,\xi,t) = G_P^q(t)\,,
\end{aligned}
$$

Nucleon Femtography

M. Burkardt PRD 62 (2000) 071503. M. Diehl EPJC 25 (2002) 223 A.V. Belitsky, D. Müller, NPA 711 (2002) 118c J.P. Ralston; B. Pire PRD 66 (2002) 111501

$$\rho_H^q(x, \boldsymbol{b}_\perp) = \int \frac{d^2\boldsymbol{\Delta}_\perp}{(2\pi)^2}\, e^{i\boldsymbol{b}_\perp\cdot\boldsymbol{\Delta}_\perp} \left[H^q\left(x, 0, -\Delta_\perp^2\right) + H^q\left(-x, 0, -\Delta_\perp^2\right)\right]$$

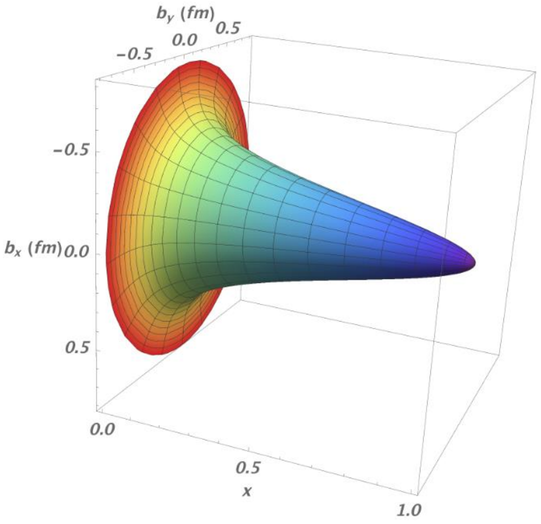

- The **transverse densities** of partons in nucleons and nuclei is related to the transverse momentum transfer ($-\Delta_\perp^2$) dependence of GPDs at **zero-skewness**.
- **DVCS** and **TCS cannot map out zero-skewness GPDs** over the **full physics phase space**.

The **experimental knowledge** of the **ξ-dependence** of GPDs at fixed longitudinal momentum fraction allows to **control** the **zero-skewness extrapolation** required for **nucleon imaging**.

Nucleon Spin

$$\lim_{t \to 0} \int_{-1}^{1} x \, [H^q(x,\xi,t) + E^q(x,\xi,t)] \, dx = J^q$$

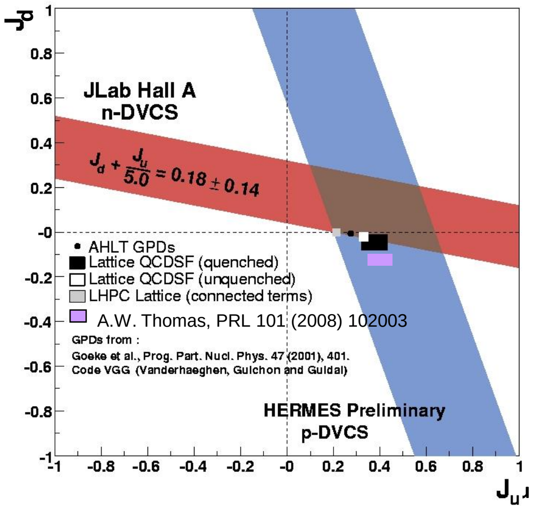

- The total angular momentum of partons inside the nucleon can be inferred from the Ji sum rule which involves the forward limit of the first Mellin moment of partons helicity conserving GPDs.
- DVCS and TCS cannot access GPDs at $x \neq \xi$ over the full physics phase space.

The experimental knowledge of the ξ-dependence of GPDs at fixed longitudinal momentum fraction is a **mandatory step for** unraveling the **nucleon spin**.

Nucleon Forces

$$\int_{-1}^{1} x \sum_q H^q(x,\xi,t)\ dx = M_2(t) + \frac{4}{5}\xi^2 d_1(t)$$

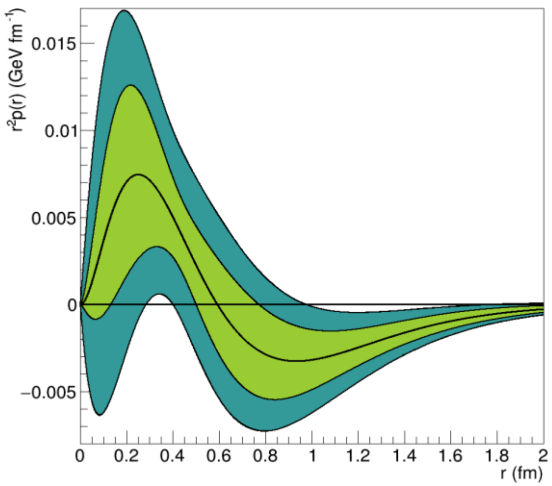

- The **skewness dependence** of the **first Mellin moment** of the GPD H provides an access to the **gravitational form factors** of the energy momentum tensor of the nucleon.
- $e^{\pm}$**-DVCS** and **TCS** offers another path via **dispersion relations**.

The **ξ-dependence** of GPDs reveals the **internal dynamics** of the nucleon.

V. Burkert, L. Elouadrhiri, F.-X. Girod, Nat. 557 (2018) 396; arXiv:2104.02031

Exclusive reaction

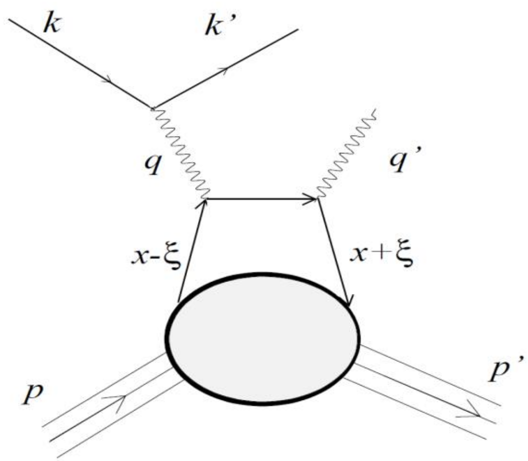

- To access GPDs, one need to study exclusive reactions
- Nucleon intact in initial and final state
- Most simple case Deeply Virtual Compton Scattering

DVCS / Double DVCS

$$\gamma^* + p \longrightarrow \gamma'(*) + p'$$

$$\hookrightarrow l^+ + l^-$$

Guidal and Vanderhaegen : Double deeply virtual Compton scattering off the nucleon (arXiv:hep-ph/0208275v1 30 Aug 2002)
Belitsky Radyushkin : Unraveling hadron structure with generalized parton distributions (arXiv:hep-ph/0504030v3 27 Jun 2005)

DDVCS cross section

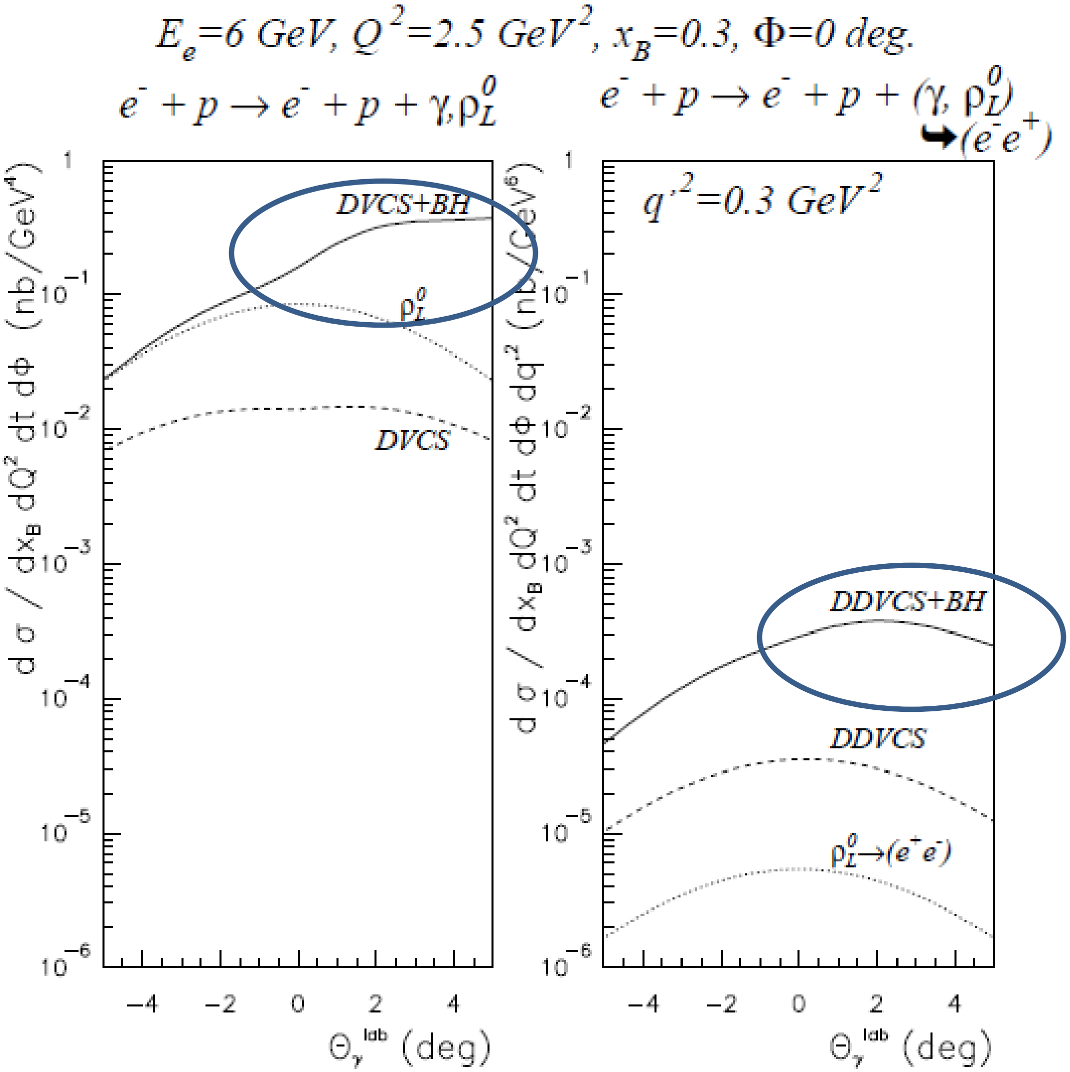

- VGG model
- Order of ~0.1 pb = 10^{-36}cm^2
- About 100 to 1000 smaller than DVCS
- Virtual Beth and Heitler
- Interference term enhanced by BH
- Contributions from mesons small when far from meson mass

Integrated Cross Section

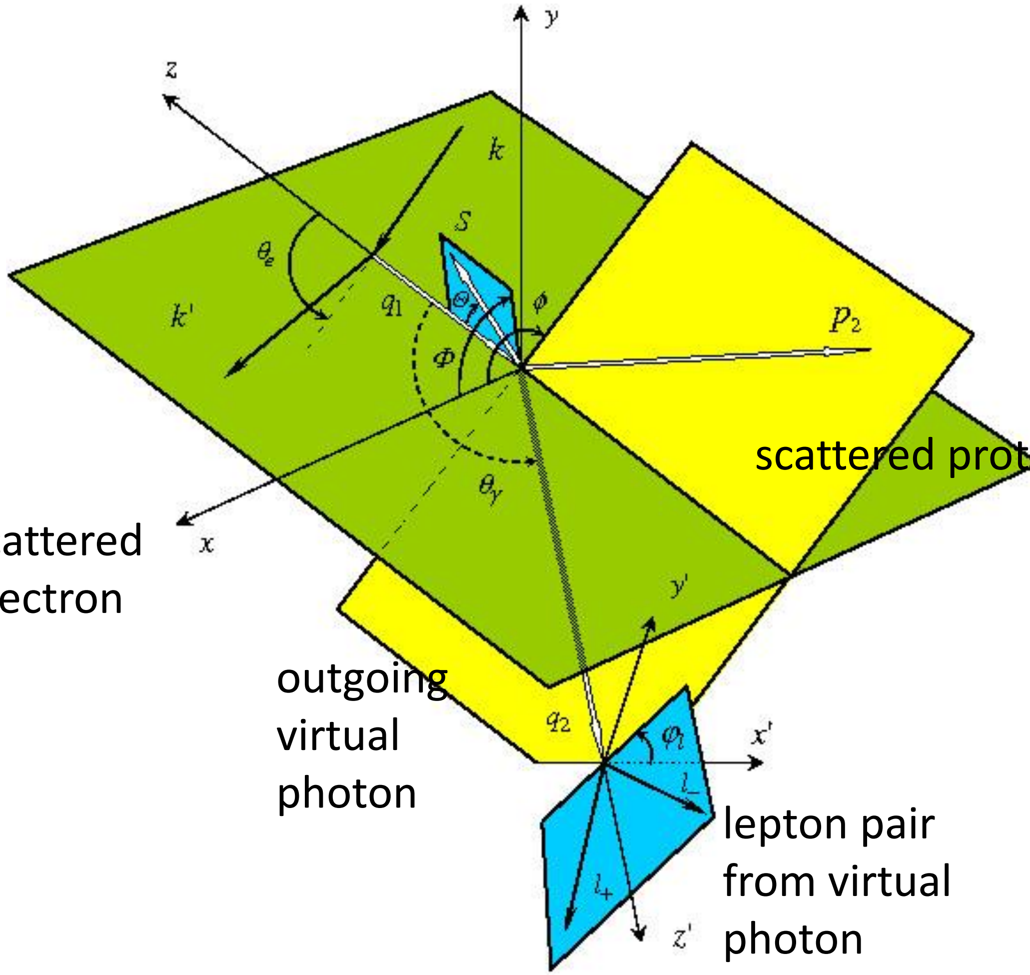

Δ = p1-p2 = q2-q1

p = p1+p2

q = ½ (q1+q2)

$Q^2 = -q^2$

$\xi' = \dfrac{Q^2}{2p.q}$ $\xi = \dfrac{\Delta.q}{p.q}$

$Q^2 = -(k-k')^2$ $x_{bj} = \dfrac{Q^2}{2p_1q_1}$

Belitsky Radyushkin : Unraveling hadron structure with generalized parton distributions (arXiv:hep-ph/0504030v3 27 Jun 2005)

$$\left\{\begin{matrix} A_{\rm LU}^{\sin\phi} \\ A_{\rm LU}^{\sin\varphi_\mu} \end{matrix}\right\} = \frac{1}{\mathcal{N}}\int_{\pi/4}^{3\pi/4} d\theta_\mu \int_0^{2\pi} d\varphi_\mu \int_0^{2\pi} d\phi \left\{\begin{matrix} 2\sin\phi \\ 2\sin\varphi_\mu \end{matrix}\right\} \frac{d^7\overrightarrow{\sigma} - d^7\overleftarrow{\sigma}}{dx_B\, dy\, dt\, d\phi\, dQ'^2\, d\Omega_\mu}$$

$$\propto \Im\mathrm{m}\left\{F_1\mathcal{H} - \frac{t}{4M_N^2}F_2\mathcal{E} + \xi(F_1+F_2)\widetilde{\mathcal{H}}\right\},$$

Integrated Cross Section

S. Zhao, PhD Thesis, Orsay (2020) K. Deja et al. PRD 107 (2023) 094035 A. Alvarado et al. arXiv:2502.02346

- **5-fold observables** obtained from the **integration over** the **polar angle** of the **muon** and the **azimuthal angle** of the **final virtual photon** are required, also **minimizing** the contribution of the BH_2 process.

$$d^5\Sigma_P^e(\varphi_\mu) = \int_0^{2\pi} d\phi \int_{\pi/4}^{3\pi/4} d\theta_{\mu^-} \ \sin(\theta_{\mu^-}) \ d^7\sigma_P^e$$

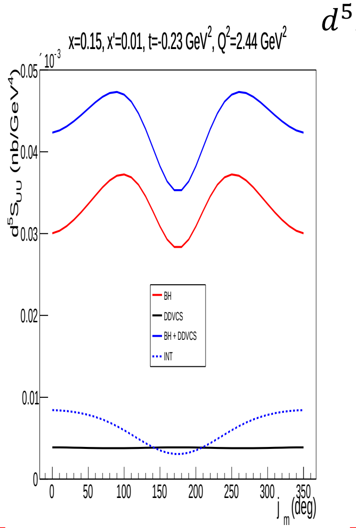

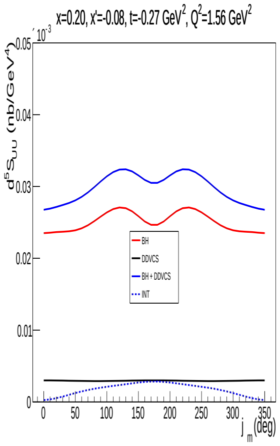

$$\boxed{d^5\Sigma_P^e = d^5\Sigma_{BH_1} + d^5\Sigma_{BH_2} + d^5\Sigma_{DDVCS} + P\, d^5\tilde{\Sigma}_{DDVCS} + d^5\Sigma_{INT_2} + P\, d^5\tilde{\Sigma}_{INT_2} - e\left[d^5\Sigma_{BH_{12}} + d^5\Sigma_{INT_1}\right]}$$

Kinematical coverage

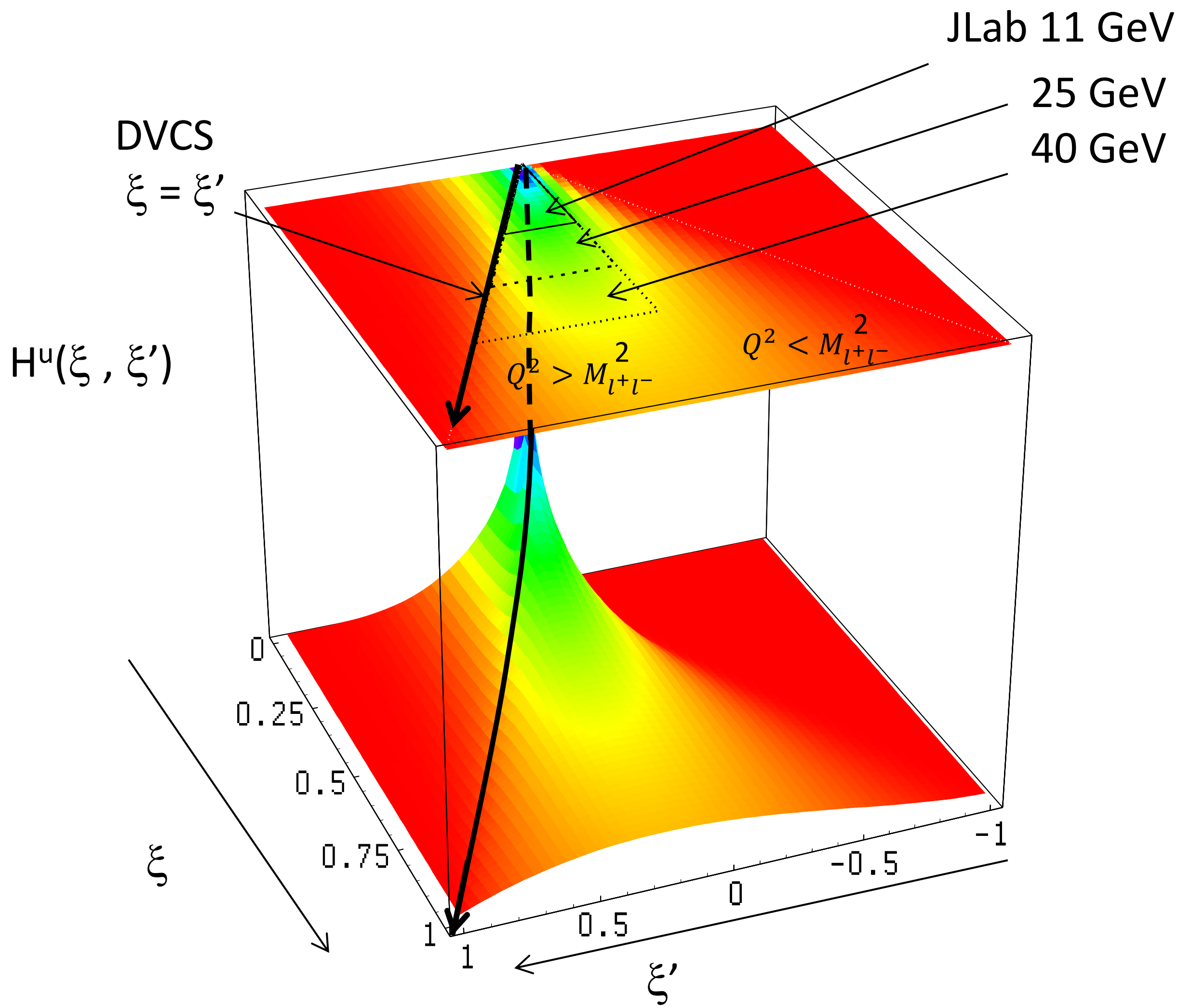

- DVCS only probes η = ξ line
- Example with model of GPD H for up quark
- Jlab : $Q^2>0$
- Kinematical range increases with beam energy (larger dilepton mass)

Experimental observables

$$\begin{Bmatrix} A_{\rm LU}^{\sin\phi} \\ A_{\rm LU}^{\sin\varphi_\mu} \end{Bmatrix} = \frac{1}{\mathcal{N}} \int_{\pi/4}^{3\pi/4} d\theta_\mu \int_0^{2\pi} d\varphi_\mu \int_0^{2\pi} d\phi \begin{Bmatrix} 2\sin\phi \\ 2\sin\varphi_\mu \end{Bmatrix} \frac{d^7\overrightarrow{\sigma} - d^7\overleftarrow{\sigma}}{dx_B\, dy\, dt\, d\phi\, dQ'^2\, d\Omega_\mu}$$

$$\propto \Im\mathrm{m}\left\{F_1\mathcal{H} - \frac{t}{4M_N^2}F_2\mathcal{E} + \xi(F_1+F_2)\widetilde{\mathcal{H}}\right\},$$

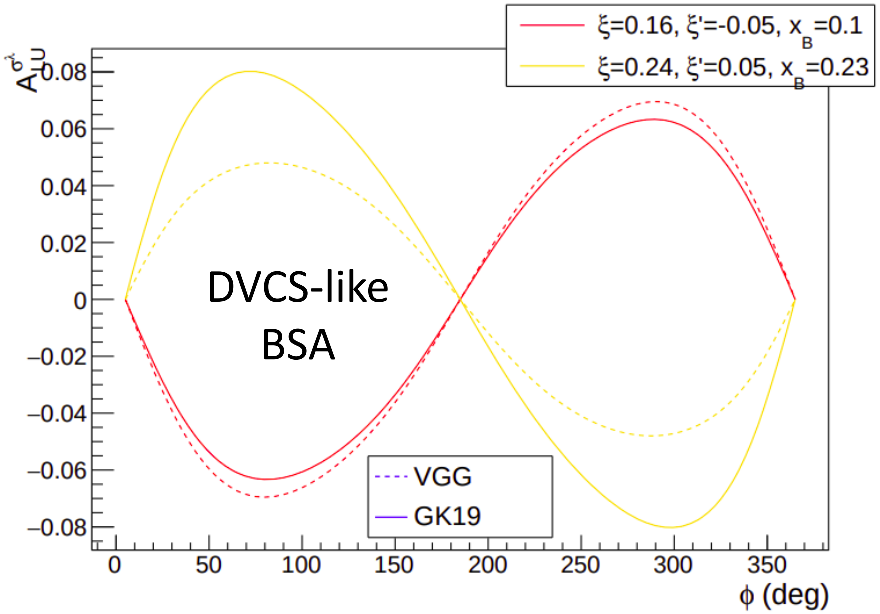

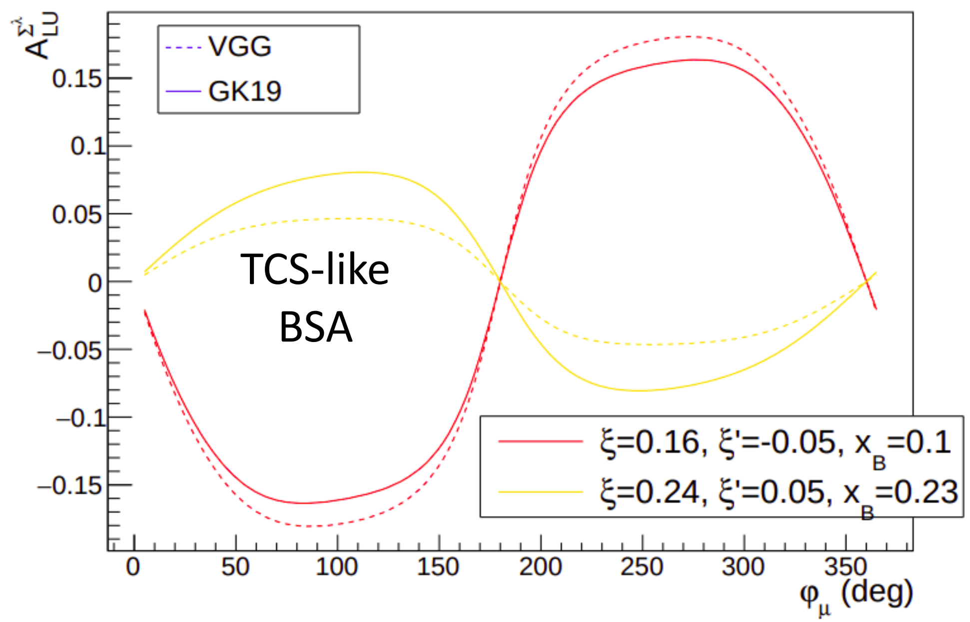

- Access to the imaginary part of CFFs.
- Sign change when transitioning from ξ'>0 ($Q^2>Q'^2$) to ξ'<0 ($Q^2<Q'^2$).
- TCS(DVCS)-like BSA enhances the amplitude in the ξ'<0(ξ'>0) region.

Experimental observables

$$\begin{Bmatrix} A_{\rm CA}^{\cos\varphi_\ell} \\ A^{\cos\varphi_\ell} \end{Bmatrix} = \frac{1}{\mathcal{N}}\int_{\pi/4}^{3\pi/4} d\theta_\ell \int_0^{2\pi} d\phi \int_0^{2\pi} d\varphi_\ell \; 2\cos\varphi_\ell \begin{Bmatrix} (d\sigma^+ + d\sigma^-)/2d\Omega_\ell d\phi \\ d\sigma^-/d\Omega_\ell d\phi \end{Bmatrix},$$

$$\propto -\frac{\xi'}{\xi}\mathfrak{Re}\left[F_1\mathcal{H} + \frac{\xi^2}{\xi'}(F_1+F_2)\tilde{\mathcal{H}} - \frac{t}{4M_N^2}F_2\mathcal{E}\right].$$

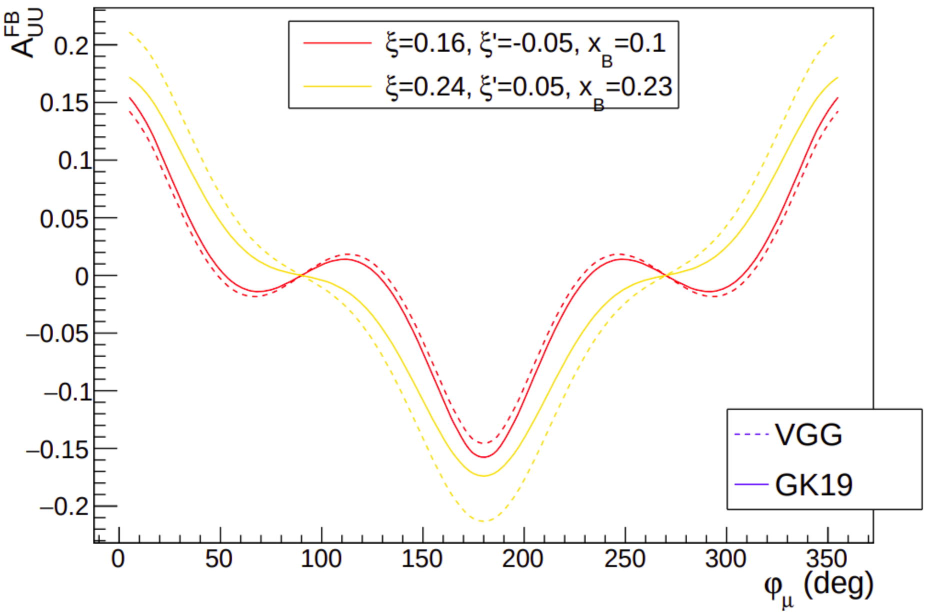

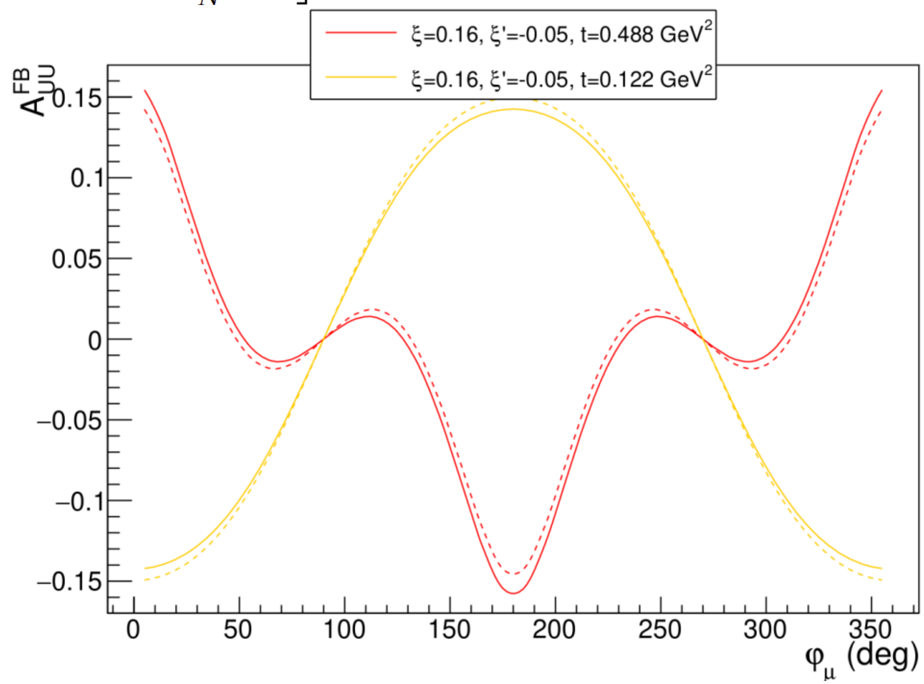

- Access to the real part of CFFs with angular asymmetries
- Curvature sign change is a highly-discriminating feature for models

Experimental observables

cosϕ moment can be accessed with the muon charge asymmetry

$$A_{UU}^{FB}(\varphi_\mu) = \frac{d^5\Sigma_{UU}(\varphi_{\mu^-}) - d^5\Sigma_{UU}(\varphi_{\mu^-}+\pi)}{d^5\Sigma_{UU}(\varphi_{\mu^-}) + d^5\Sigma_{UU}(\varphi_{\mu^-}+\pi)} = \frac{d^5\Sigma_{UU}(\varphi_{\mu^-}) - d^5\Sigma_{UU}(\varphi_{\mu^+})}{d^5\Sigma_{UU}(\varphi_{\mu^-}) + d^5\Sigma_{UU}(\varphi_{\mu^+})} = A_{UU}^{\mu^\pm}(\varphi_\mu)$$

$$A_{UU}^{\mu^\pm}(\varphi_\mu) = \frac{d^5\Sigma_{BH_{12}} + d^5\Sigma_{\mathcal{I}_2}}{d^5\Sigma_{BH_1} + d^5\Sigma_{BH_2} + d^5\Sigma_{DDVCS} + d^5\Sigma_{\mathcal{I}_1}}$$

$$\frac{d^4\sigma_{INT}}{dQ'^2 dt d\Omega} = -\frac{\alpha_{em}^3}{4\pi s^2}\frac{1}{-t}\frac{m_p}{Q'}\frac{1}{\tau\sqrt{1-\tau}}\frac{L_0}{L}[\cos(\phi)\frac{1+\cos^2(\theta)}{\sin(\theta)}\mathrm{Re}\tilde{M}^{--}$$
$$\cancel{-\cos(2\phi)\sqrt{2}\cos(\theta)\mathrm{Re}\tilde{M}^{0-}} + \cos(3\phi)\sin(\theta)\mathrm{Re}\tilde{M}^{+-} + O(\frac{1}{Q'})],$$

- There are contributions from cos(ϕ) and cos(3ϕ) modulations to the µCA.
- cos(ϕ) can be extracted from fits
- As BH is known, it can be subtracted

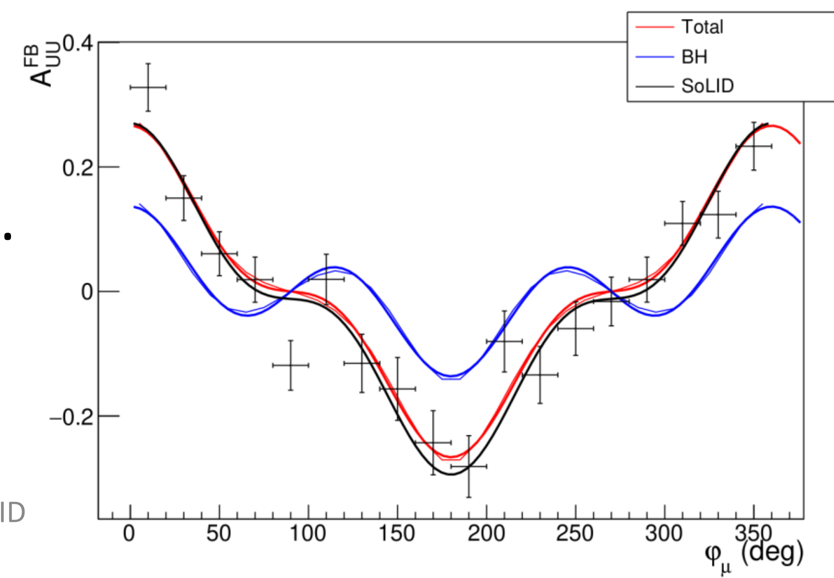

Experimental Setup

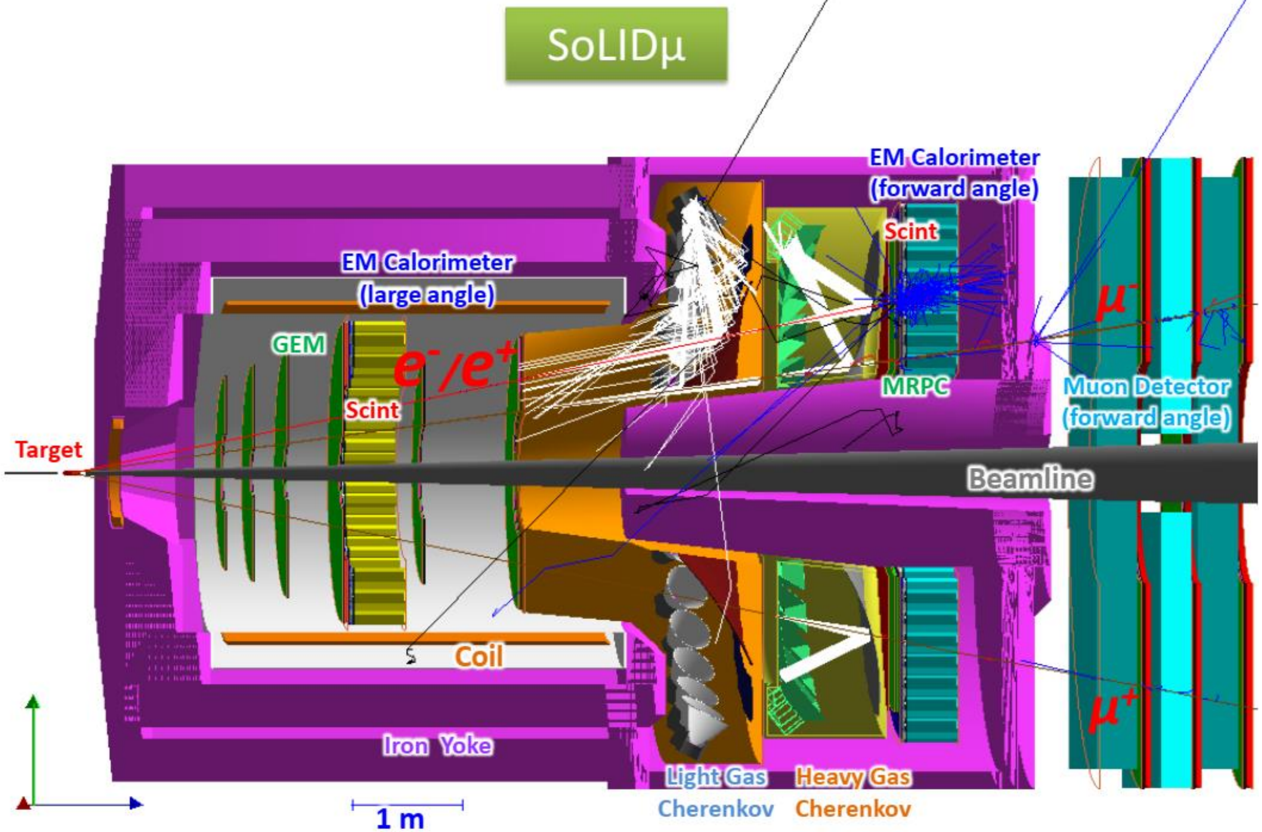

- Based on SoLID J/Psi and TCS setup with forward angle muon detector added
- Sharing beam time with added muon channels for J/Psi and TCS
- Forward Angle (FA) covers 8.5-16.5deg and Large Angle (LA) covers 18-30deg

Forward Angle Muon Detector (FAMD)

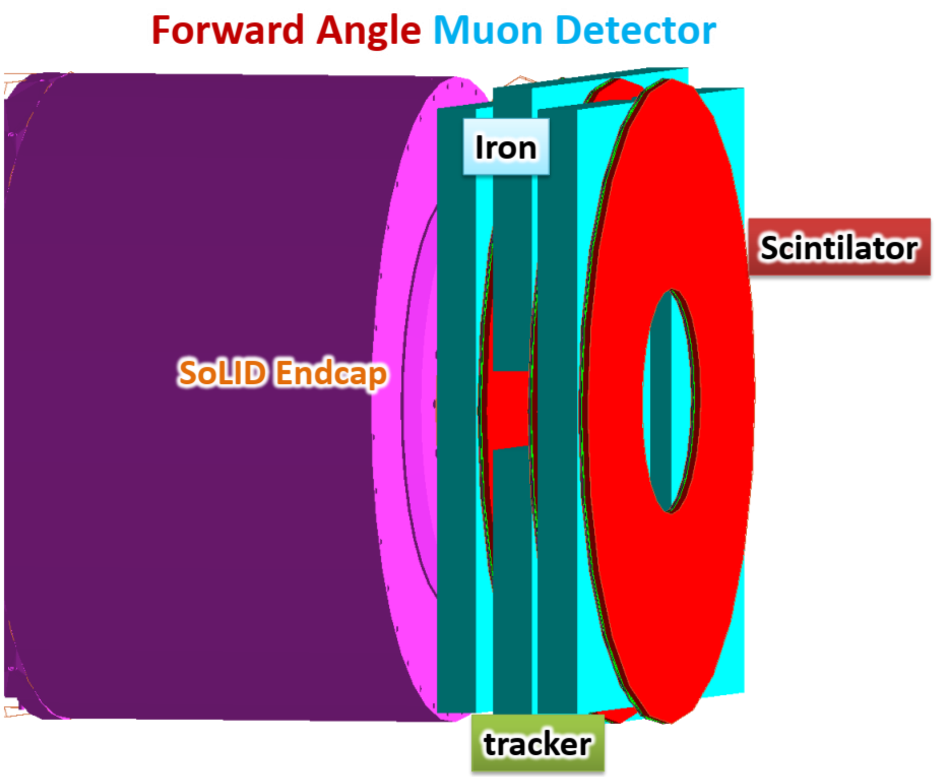

- 3 layers of iron for pion blocking
- 3 layers of μRWell trackers for tracks in FAMD to connect with tracks in SoLID inner GEM trackers
  - track resolution from SoLID inner trackers only
- 3 layers of scintillators for pion suppression and muon PID. And last layer for trigger

Iron of FAMD

- Reuse 6 of 8 CLEO octagon outer layer iron
- Each one is about 36x254x533cm
- No problem with space
- Field (<10G),force(<1N),torque(<2Nm) are small

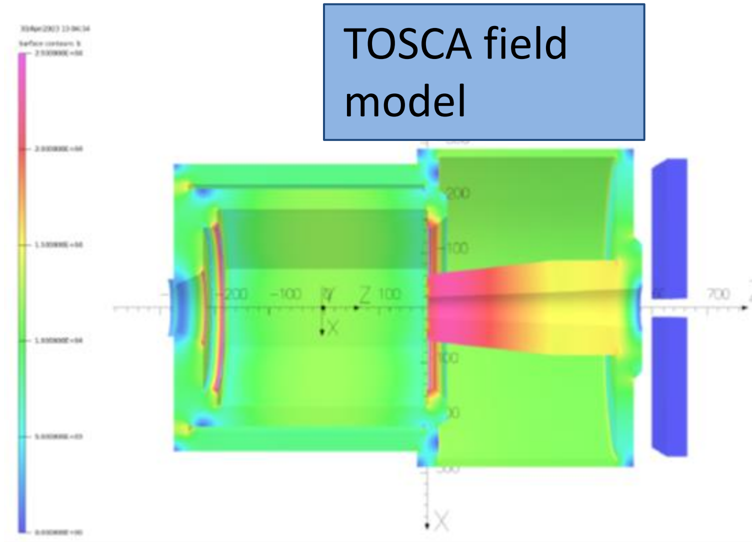

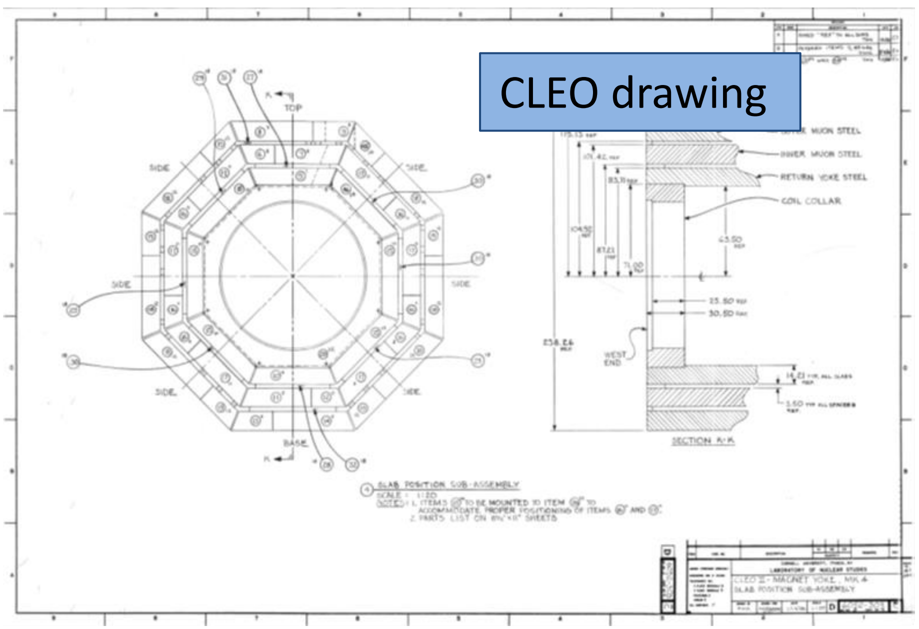

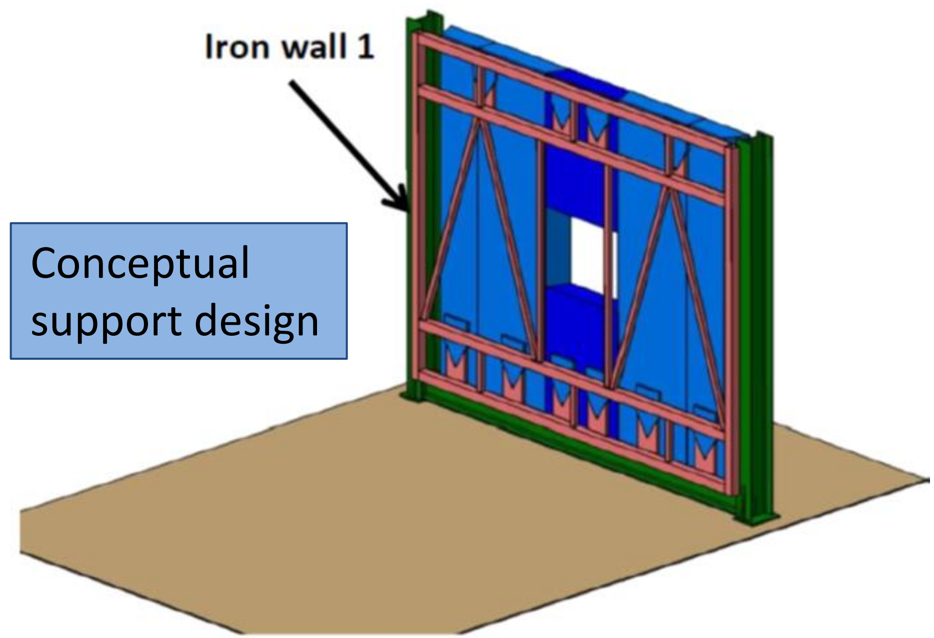

µRWell trackers of FAMD

- µRWell with good rate capability and lower cost than GEM
- VMM electronics
- 2D UV strips with capacitive charge sharing to have rate 30KHz/cm2 and position resolution of 1 mm

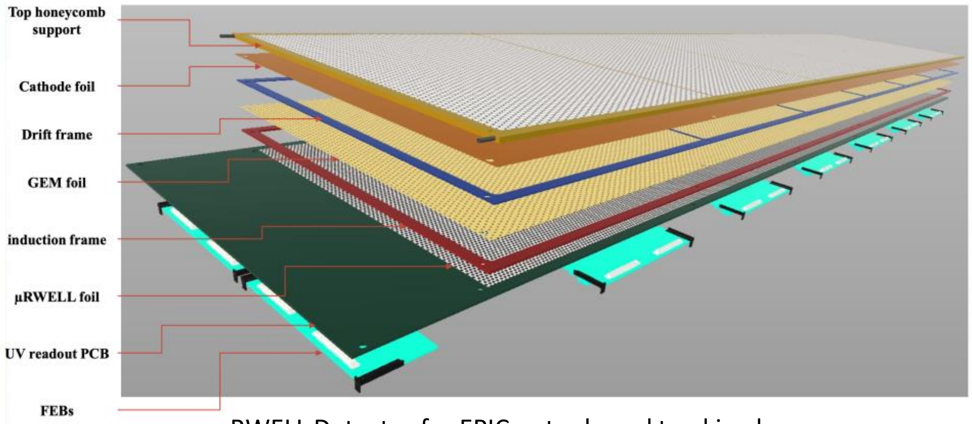

μRWELL Detector for EPIC outer barrel tracking layer

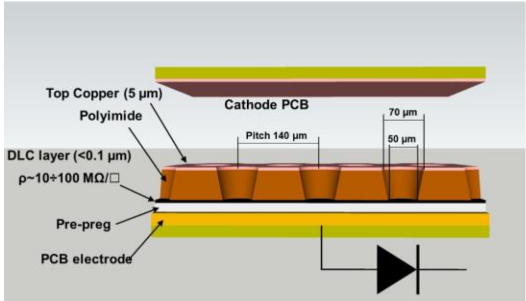

μRWELL Detector – G. Bencivenni *et al* 2019 *JINST* **14** P05014

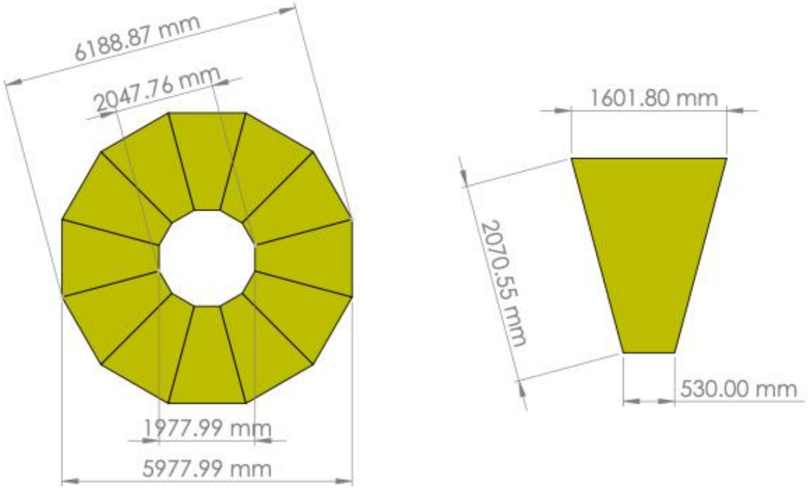

A plane of μRWELL detectors for muon detection

Scintillators of FAMD

- Each plane has 60 azimuthal segments
- Readout with light guide and PMTs from both inner and outer radial ends
- Thickness 5cm and 150 ps time resolution
- Design similar to CLAS12 forward scintillator and SoLID large angle scintillator with similar performance

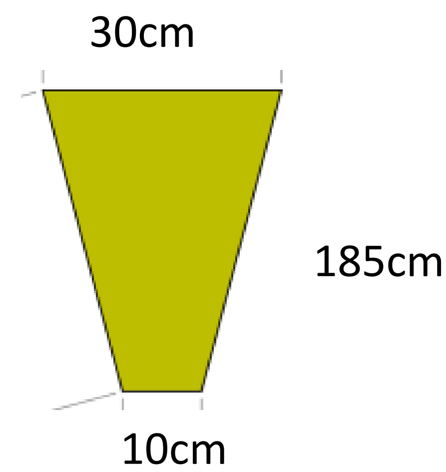

Event Acceptance

BH generator "grape-dilepton" used by HERA and verified by CLAS12

- Best topology 3fold(e+mu+mu): scattered e- at FA+LA, both muons at FA, proton not detected (shown below)
- Additional topology 4fold(e+mu+mu+p): scattered e- and recoil proton at FA+LA, both muons at FA

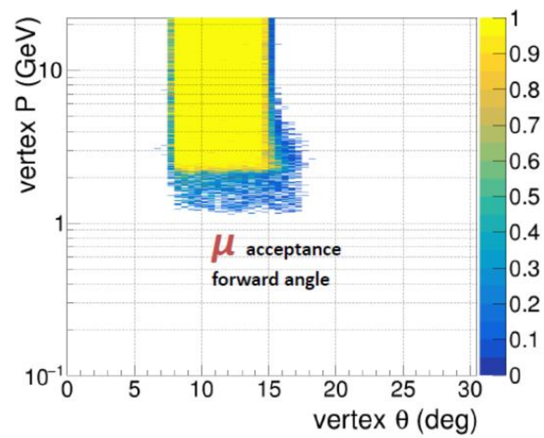

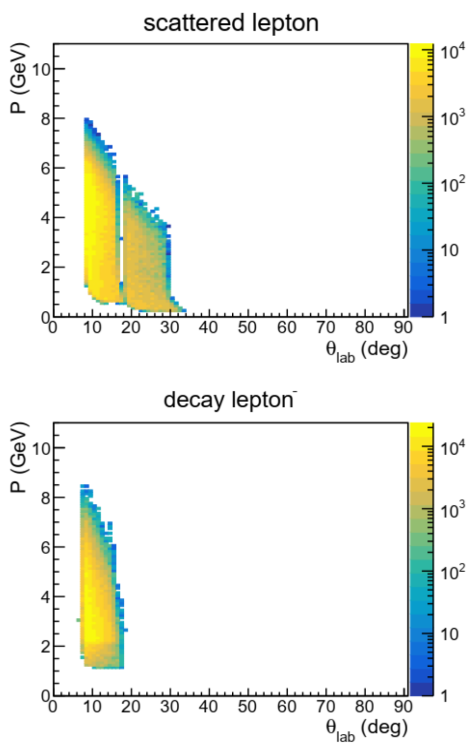

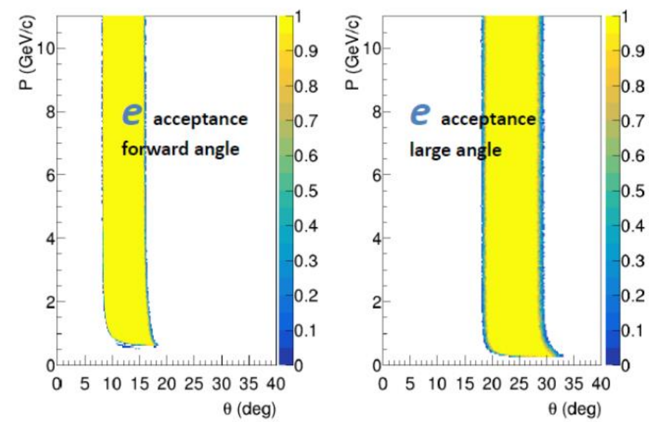

Event Distribution

BH generator "grape-dilepton" used by HERA and verified by CLAS12

- 3fold BH events covers large kinematic range
- 0.7 overall detection efficiency
- Enough counts for 1.2e37/cm2/s lumi and 100 days to have multidimensional binning

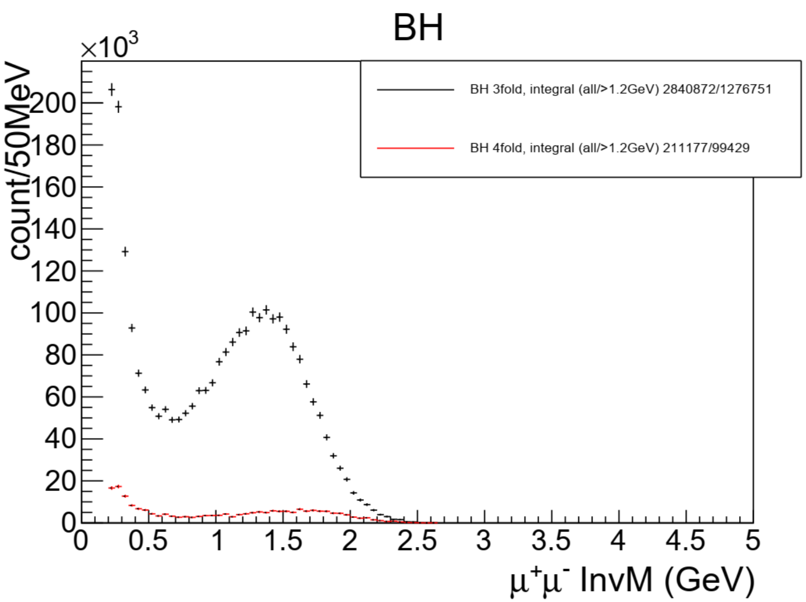

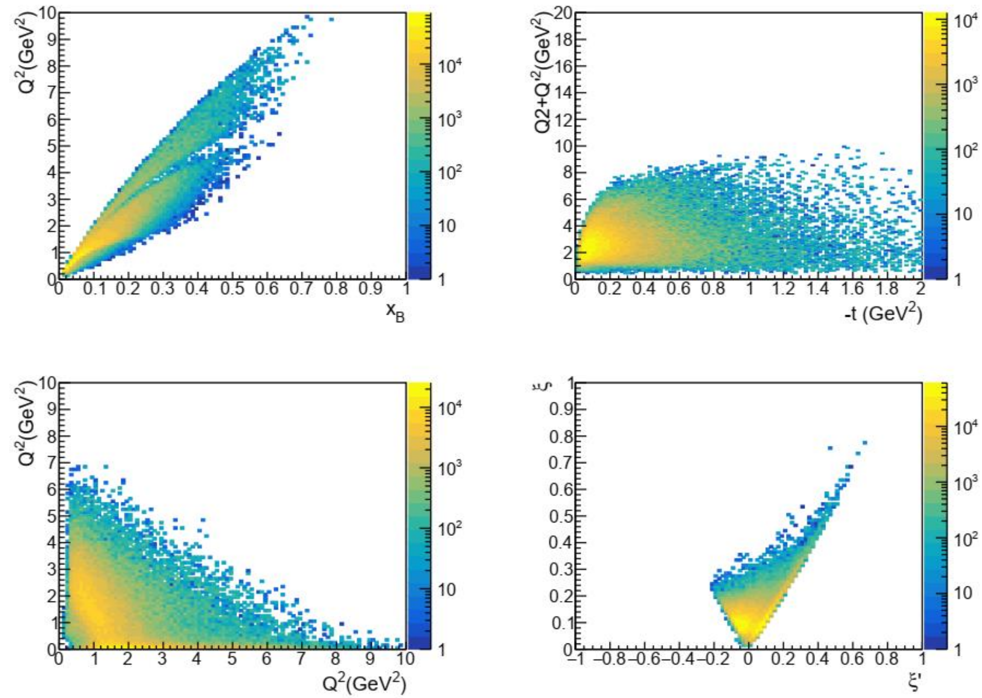

Exclusivity cut

- Both BH with 4 final particles (elastic) and more than 4 particles (quasi-elastic) are generated by "grape-dilepton"
- Missing proton mass of 3 fold BH events with resolution from SoLID inner GEM trackers, for resonance free region (muon pair InvM>1.2GeV)
- 3-4% background left after cutting MM>1.15GeV

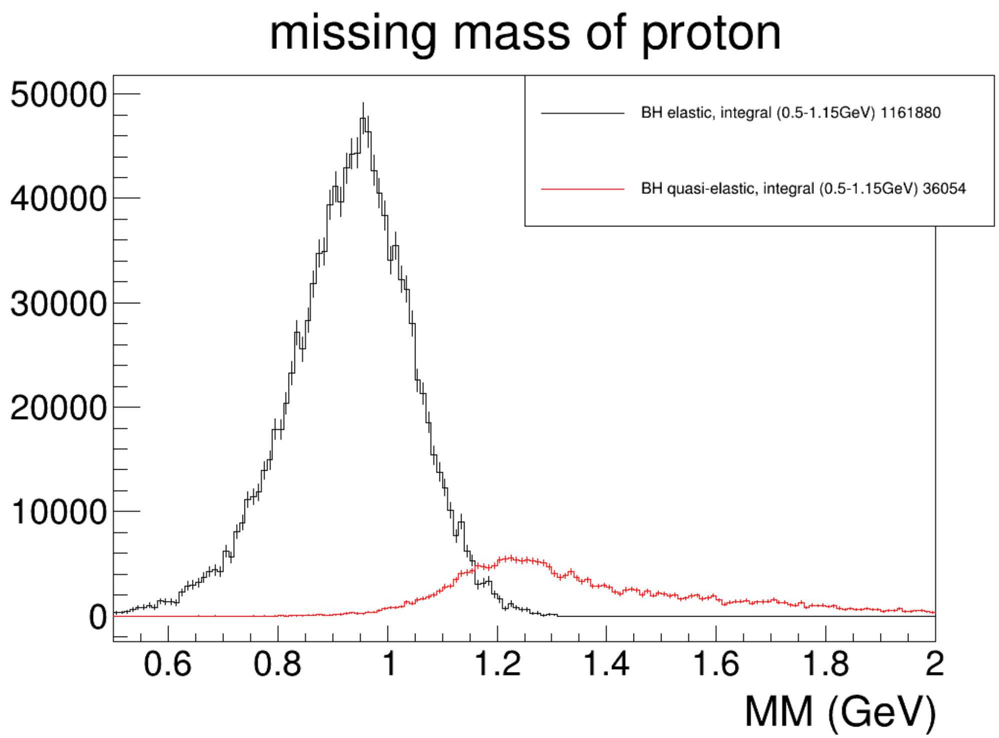

Pion blocking

- Geant4 simulation of pions from target with some probabilities creating hits at FAMD
- "pion hit probability", hits of charged particles entering each layer, used for FAMD detector and trigger rate estimate
- "pion surviving probability", hits of pion and muon at the last layer of FAMD and a track passing all SoLID inner GEM trackers, used for physics event rate estimation

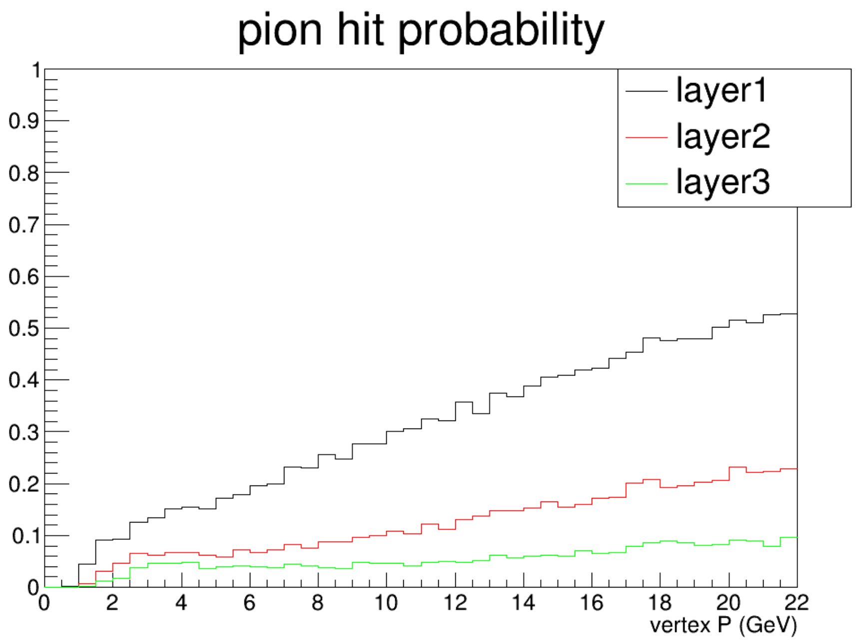

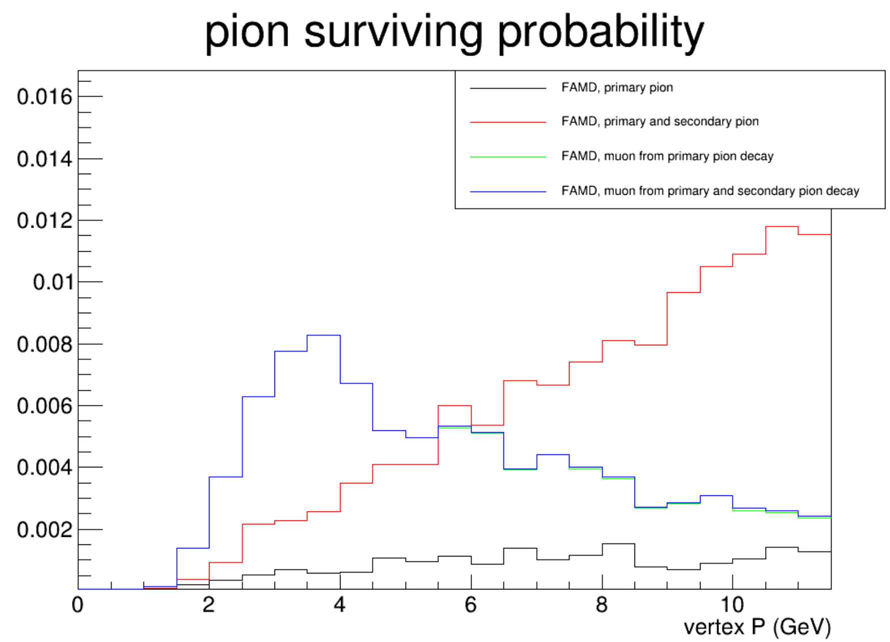

Pion rejection within FAMD

- Muons behave as Minimum Ionizing Particle (MIP)
- Pions often deposit more energy over 3 layers of scintillators.
- Use moderate pion suppression factor 2 from energy cut

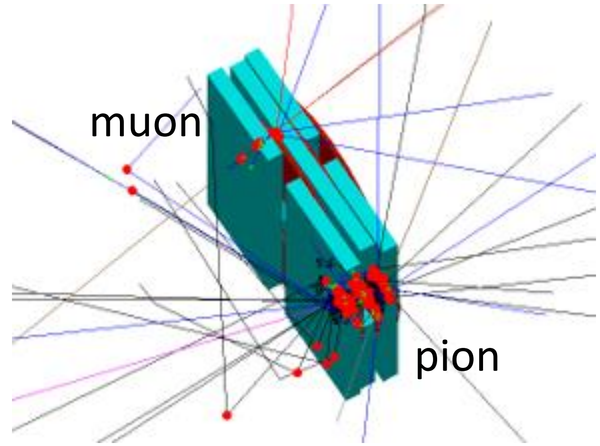

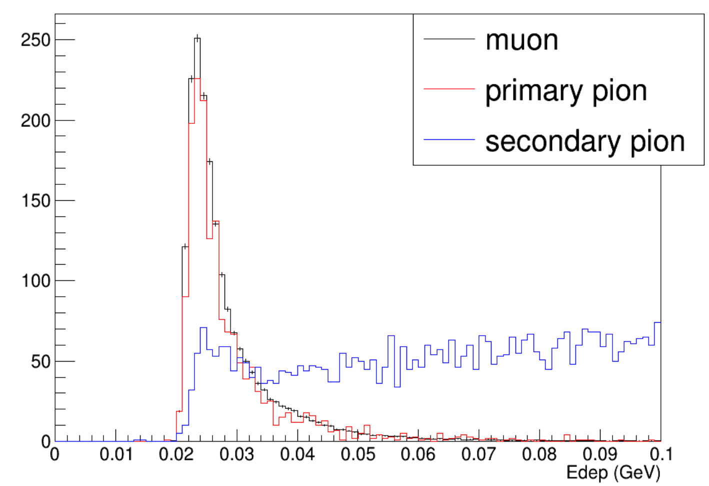

Single pion background

- Combining single pion generator "evgen_bggen" (pythia+MAID) events with "pion hit probability", study charged particle rate at 3 layers
- Adding a safety factor 2 to obtain single particle trigger 600khz rate at the last layer of scintillator. Coincidence of two hits from 2 different sectors (out of total 60 sectors) within 50ns time windows leads to 18khz final trigger rate
- Full simulation confirmed the result

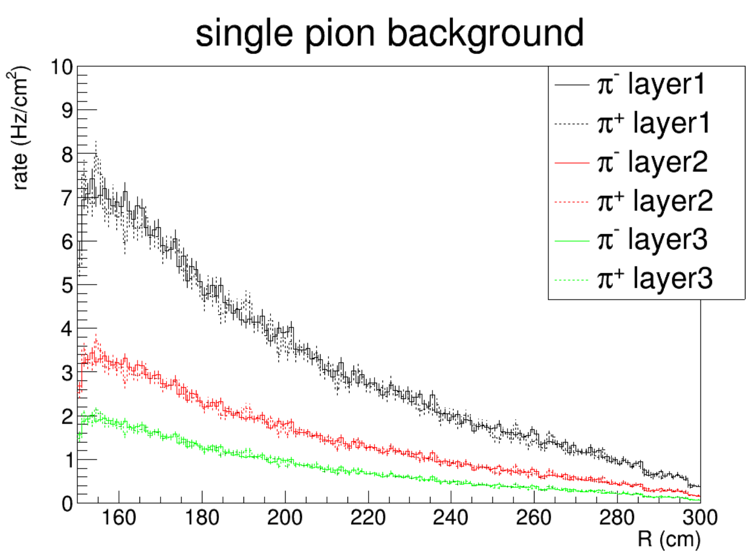

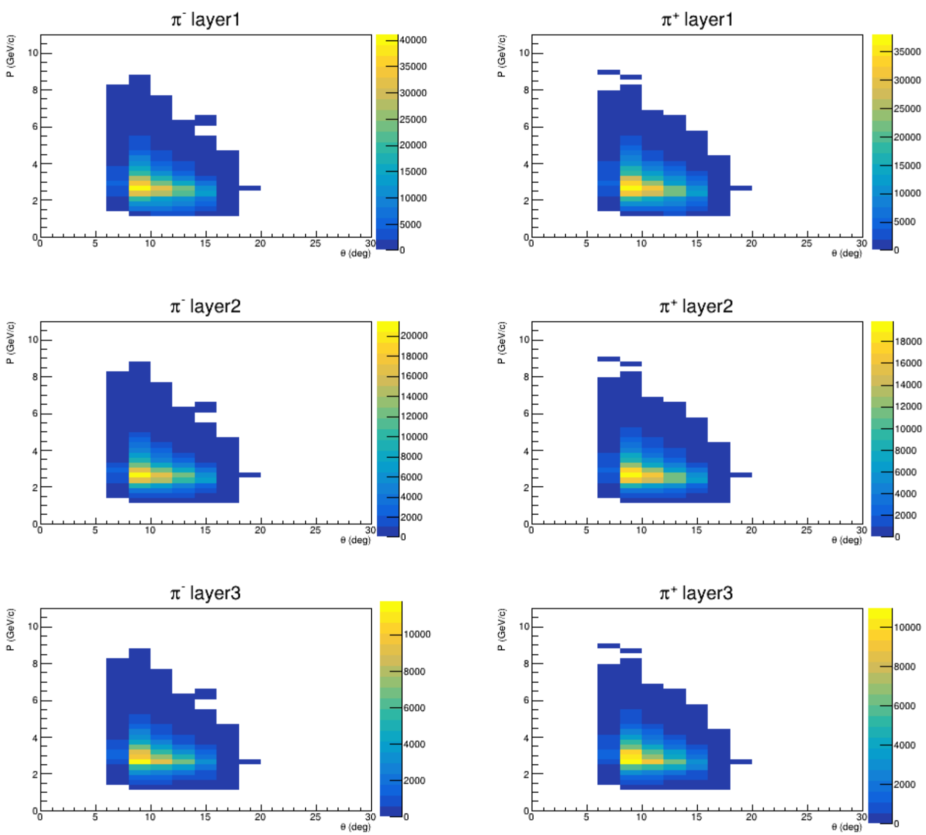

Two pion exclusive background

- Main physics background from two pion exclusive channel (missing mass cut won't reject it because of pion and muon have similar mass)
- Combine event generator "twopeg" (fit to CLAS data) and "pion hit probability" with pion suppression factor 2, study "2pi" rate and compare to BH rate
- 5-7% background

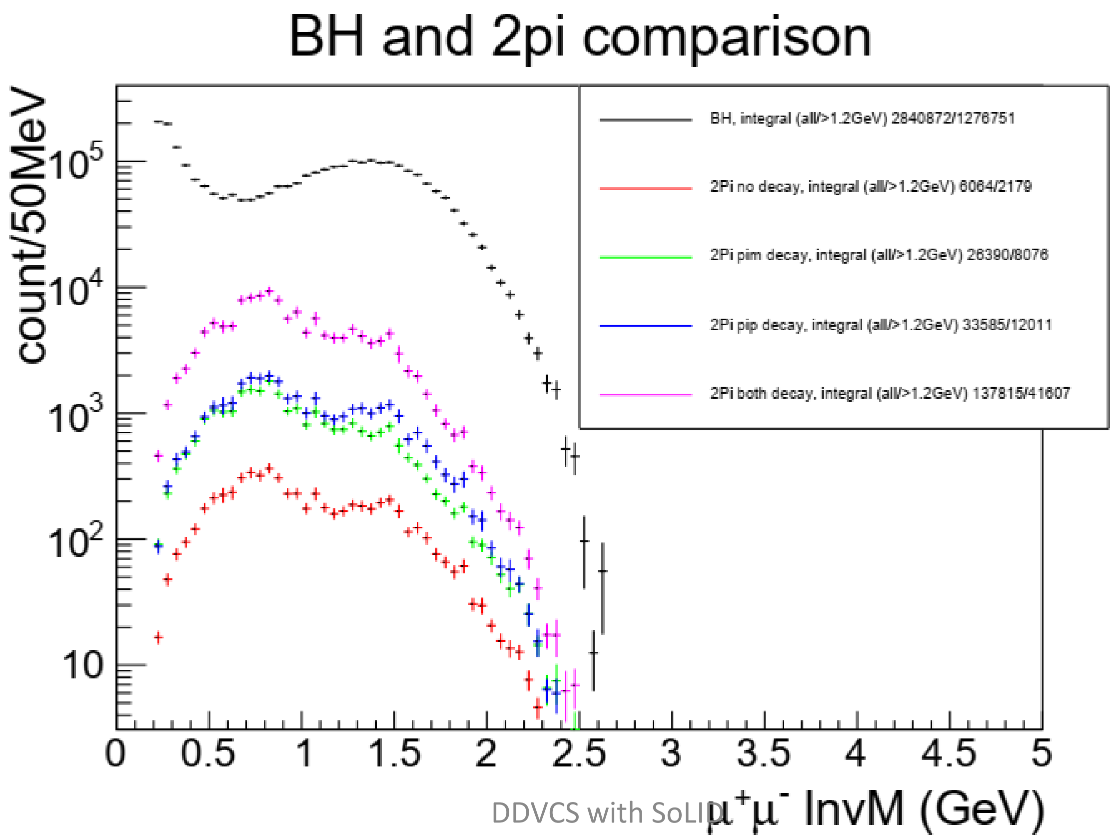

Experimental projections

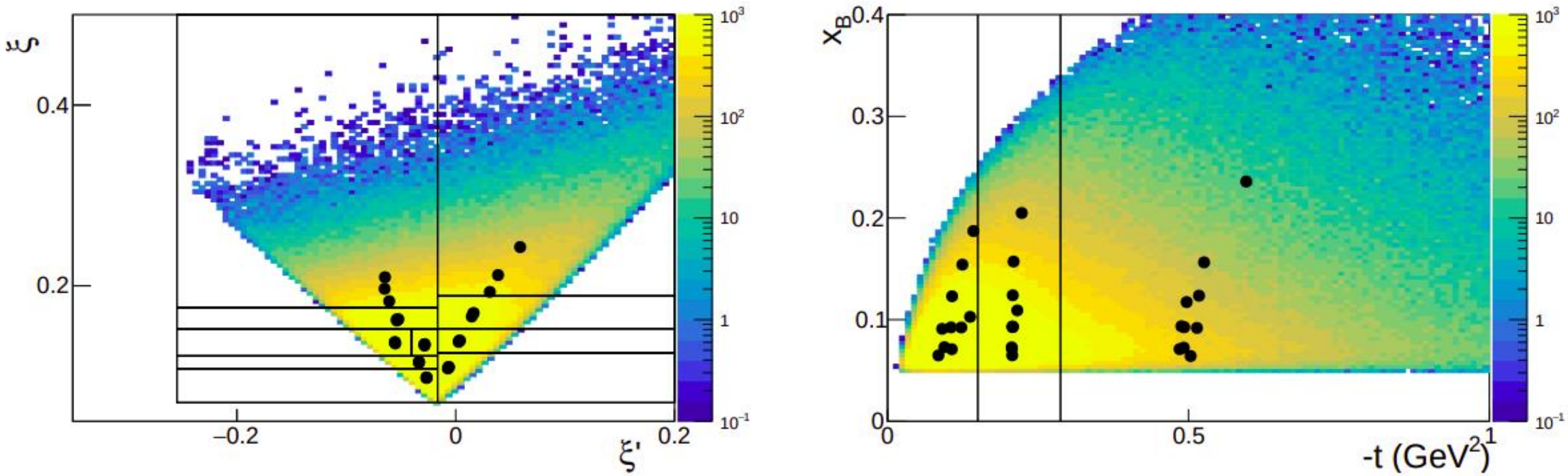

(a) (ξ', ξ) space. (b) $(-t, x_B)$ space.

- 100 days would allow for exploratory measurements on a five-dimensional grid.

BSA experimental projections

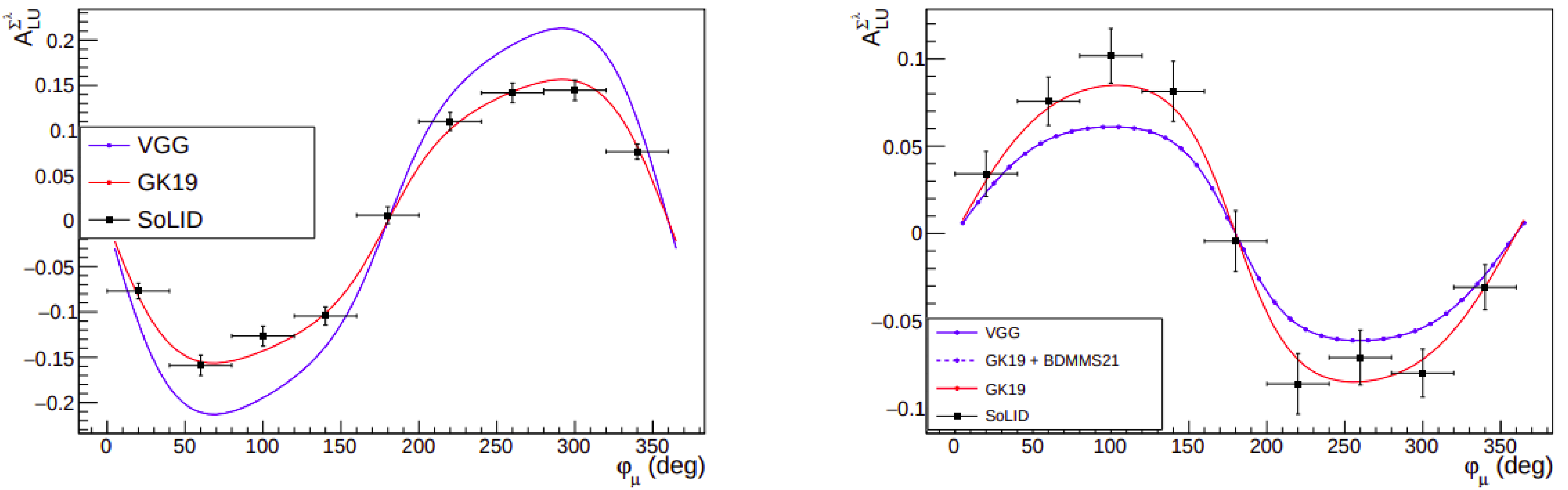

(a) TCS-like BSA in the TCS-like region (Bin 21).

(b) TCS-like BSA in the full DVCS-like region.

Figure 25: Sample TCS-like BSA projections.

- First-time measurements of the BSA sign change
- Possibility to constrain GPD models

μCA experimental projections

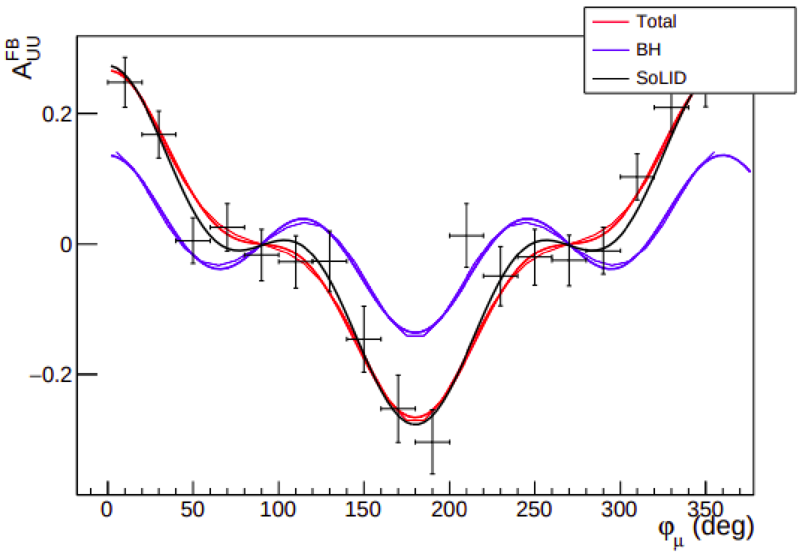

(a) μCA and the components entering the $\cos\varphi_\mu$ moment.

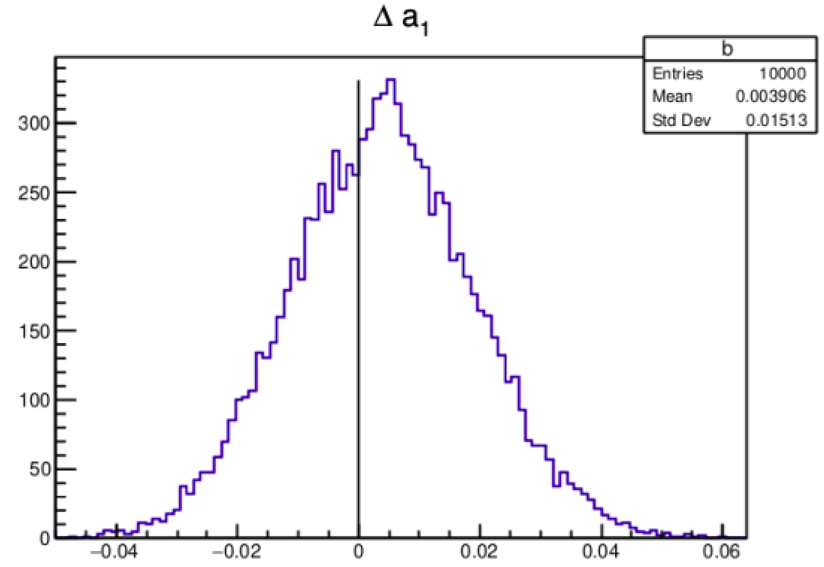

(b) Distribution of the $\cos\varphi_\mu$ moment of the μCA after 10k iterations.

Figure 28: Extraction of $\cos\varphi_\mu$ moment of the μCA on bin 13.

Sample cos(ϕ) extraction with a 11% error.

μCA experimental projections

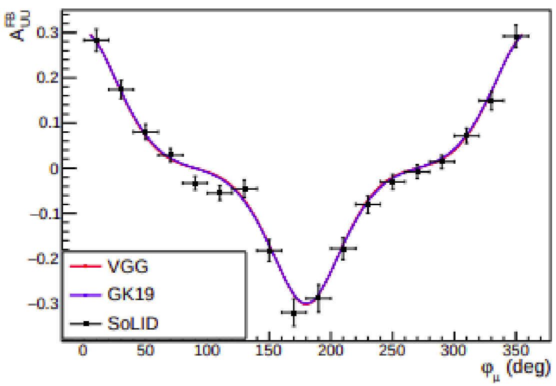

(d) Bin 19.

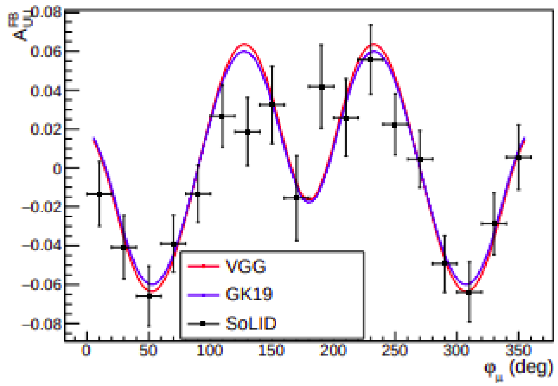

(e) Bin 20.

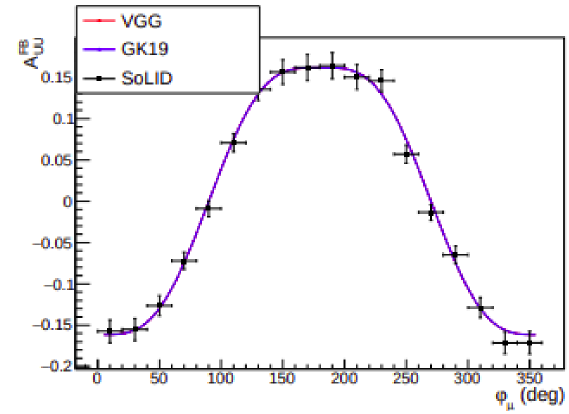

(f) Bin 21.

- Observation of the CFF real part curvature change

Beam time request

Beam Energy (GeV)	Beam Current (uA)	Beam Requirements	Target Material	Target Thickness (cm)	Beam time (days)
11	3	polarized (>85%)	LH2	15	
Run Group Calibration time					10
Run Group Production time					50
Requested Production time					50
Total Time					110

Summary

- We are proposing to complement the J/Psi SoLID setup with a muon detector
- This will allow us to measure DDVCS in the dimuons channel
- We will use the J/Psi beamtime and will request additional 50 days to measure the DDVCS asymmetries

Backup

Muon Detector

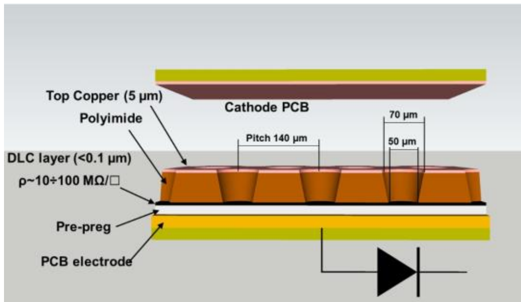

μRWELL Detector – G. Bencivenni *et al* 2019 *JINST* **14** P05014

- Utilize μRWELL detectors for muon tracking layers
  - Current μRWELL detector rate capability – ~200 KHz/cm^2 (High-rate version in development – 10 MHz/cm^2)
  - Discharge resistant thanks to integrated DLC layers – a huge improvement on electronics stability – less interruption on DAQ during running
  - No spacers needed compared with GEM detectors – no dead area
- A similar technology adopted by EIC
  - Our muon detector unit would be roughly in the same size as EIC prototypes
  - Total cost (3 complete layers covering a total of 75 m^2) around 900K

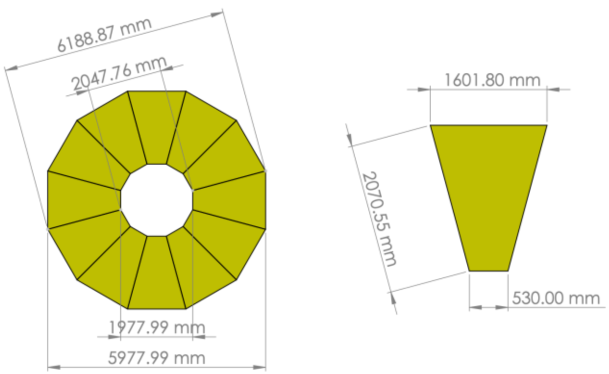

A plane of μRWELL detectors for muon detection

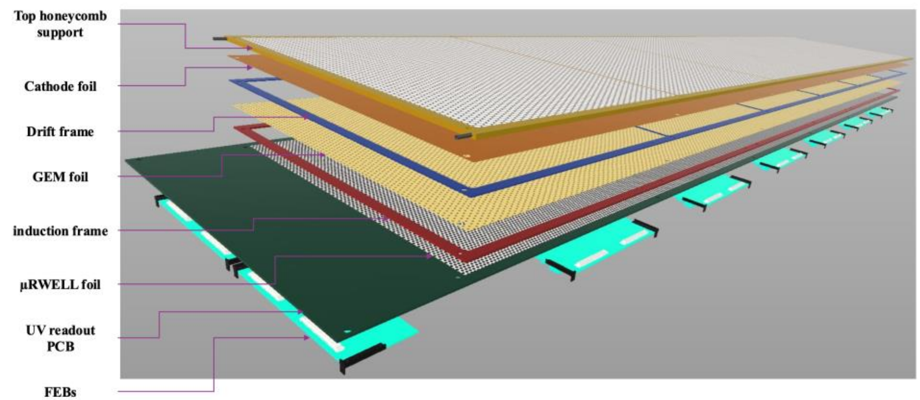

μRWELL Detector for EPIC outer barrel tracking layer

Muon Detector

- Use capacitive charge sharing technique to reduce total readout channels while maintain the same space resolution
- Works for all readout patterns – strip, pad, zigzag, …

With Capacitive charge sharing:

- Space resolution : 1 mm
- Total readout channel can be reduced to around 22K for all 3 layers combined
- Detector rate will be determined by the final readout strip width, larger strip width leads to lower detector rate capability
- For 22K readout channels, 1 mm space resolution, with capacitive charge sharing technique – rate capability: $\sim 30\ KHz/cm^2$ (assume 300 ns signal integral time)

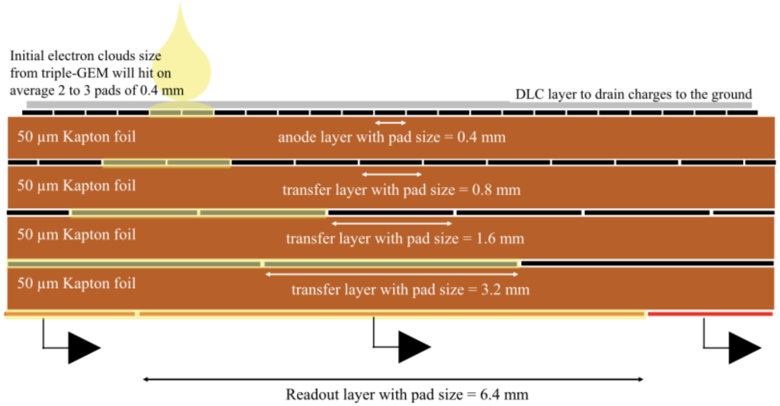

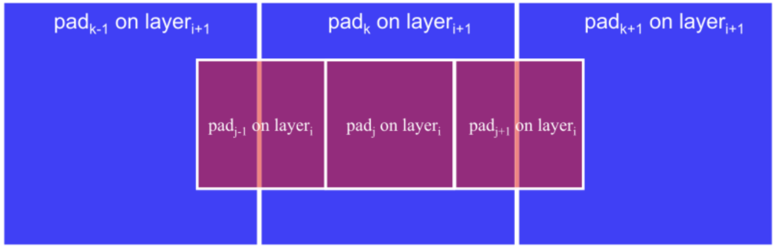

Concept for capacitive charge sharing – K. Gnanvo *et al, Nuclear Inst. and Methods in Physics Research, A 1047 (2023) 167782*

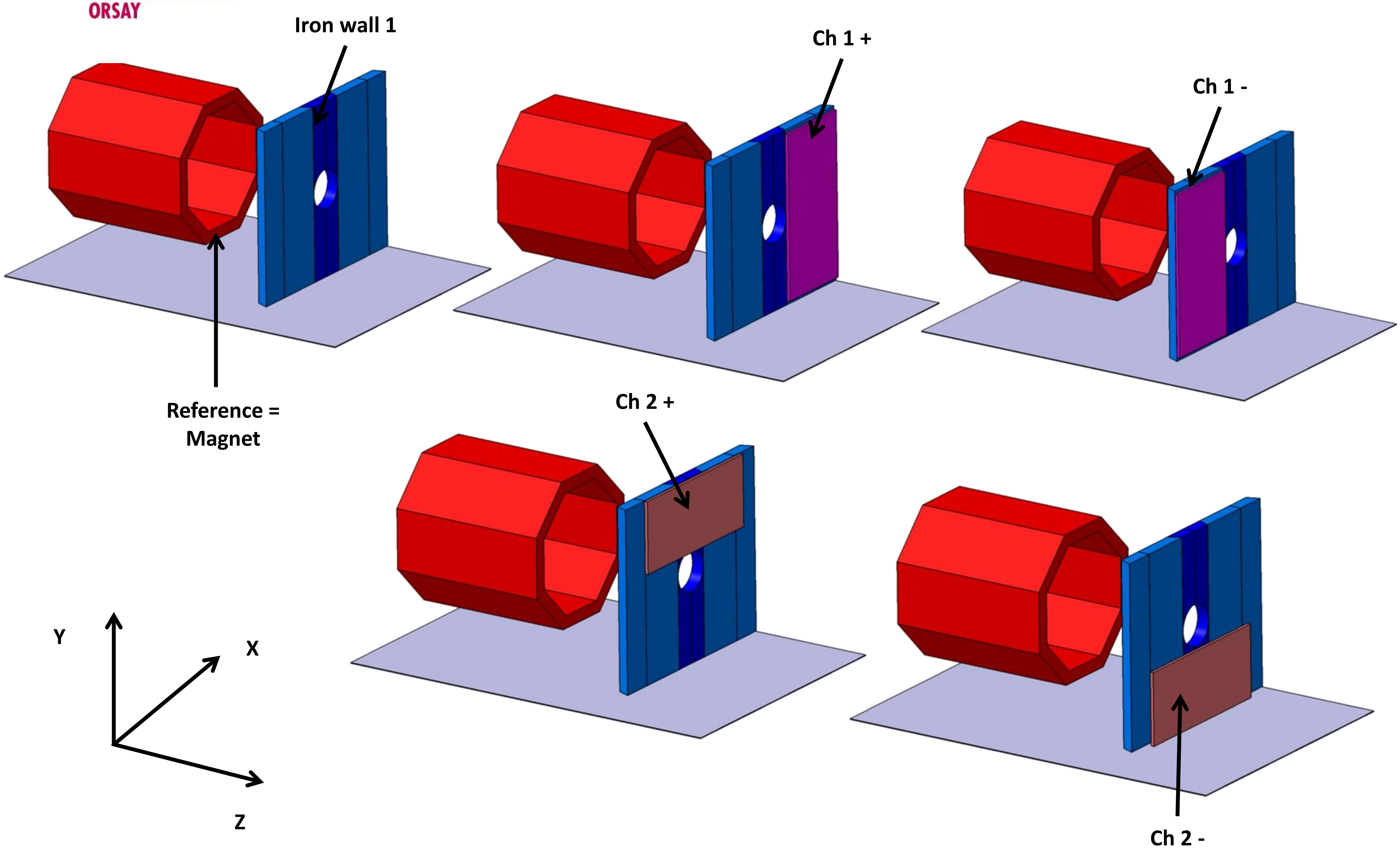
Iron wall 1
Ch 1 +
Ch 1 -
Reference =
Magnet
Ch 2 +
Y
X
Z
Ch 2 -

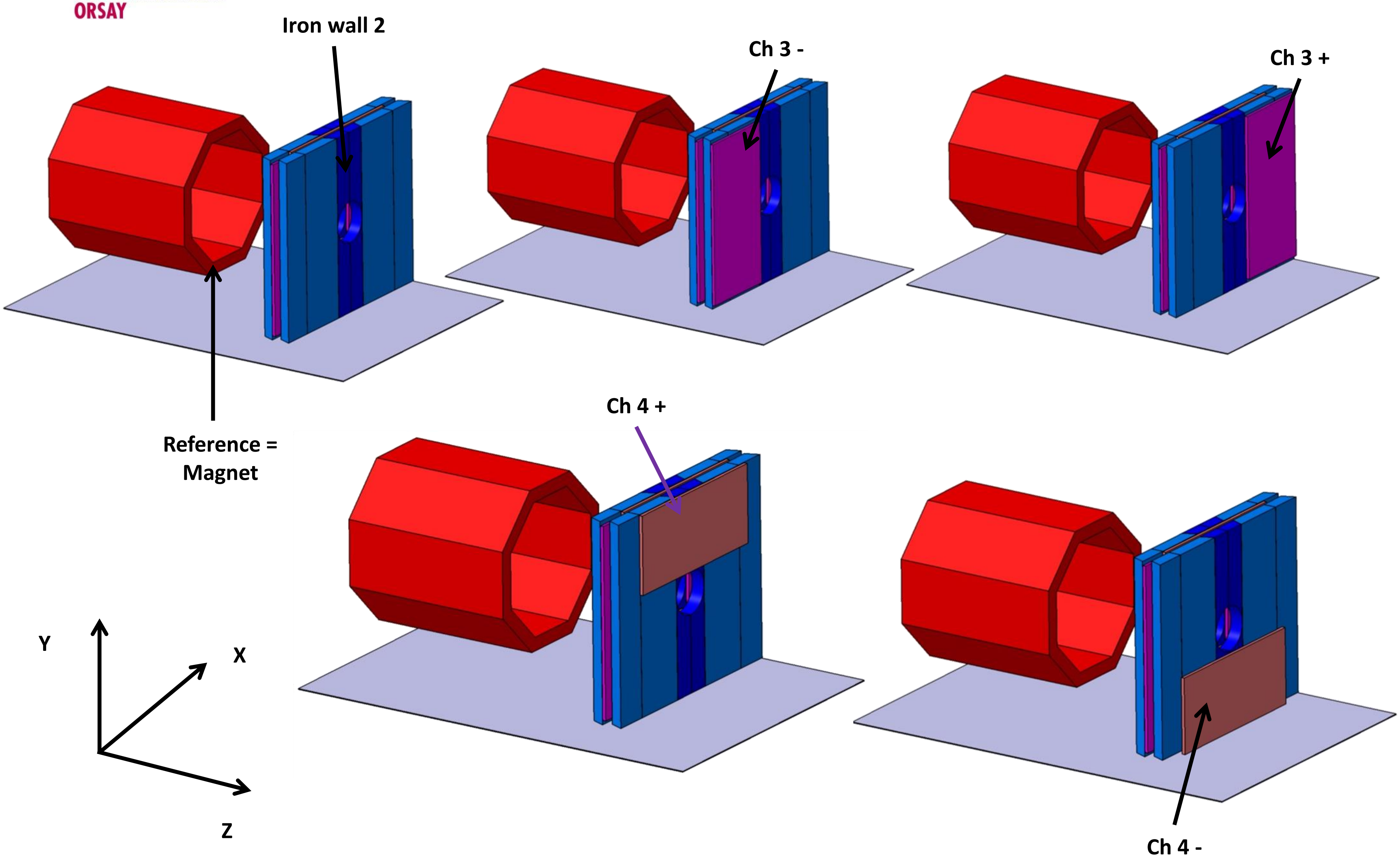
Iron wall 2
Ch 3 -
Ch 3 +
Reference =
Magnet
Ch 4 +
Ch 4 -
Y
X
Z

Higher luminosity J/Psi setup tracking study

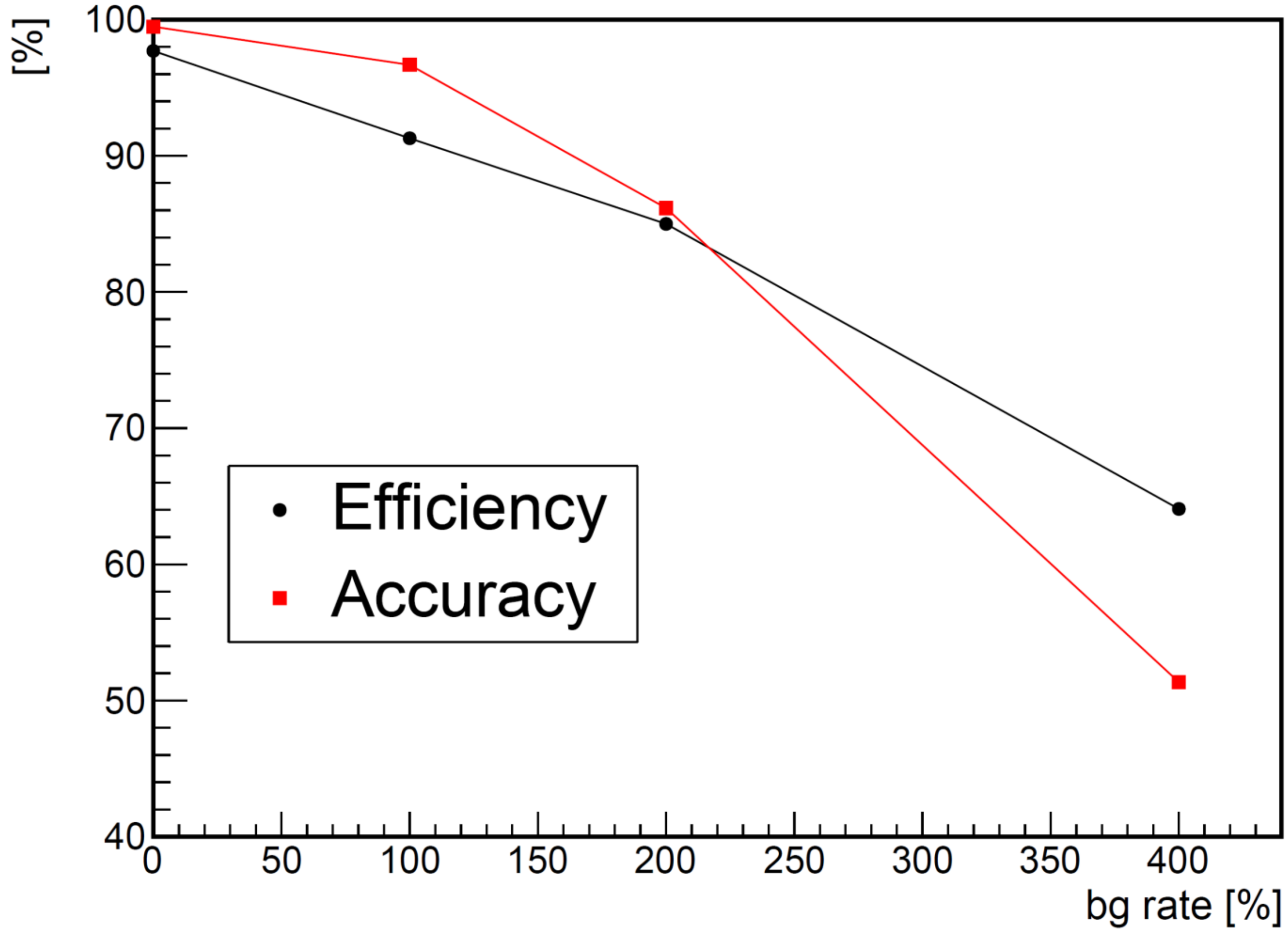

Weizhi Xiong

Simple Kalman filter tracking

Higher luminosity ?

- Current could go up to 80 uA
- Target length up to 1 meter (~1.8 10^39 $cm^{-2}s^{-1}$)
- Tracker occupancy and photon background
  - Reduce amount of Copper in GEM
  - Micromegas option
  - Build smaller chambers and add more channels
  - Study complement with 2D pad readout
  - Superconducting tracker option
  - Radiation hardened silicon and MAPS
- Calorimetry
  - Study liquid scintillator and cryogenics calorimeter option
  - Superconducting detector to replace PMT (1 ns width pulse to increase rate capability)
- Cerenkov
  - Superconducting detector to replace PMT (1 ns width pulse to increase rate capability)
  - HBD type Cerenkov for Large Angle calorimeter

6. 10^38 $cm^{-2}s^{-1}$

Technically doable mostly matter of cost

Kinematical coverage 11 GeV

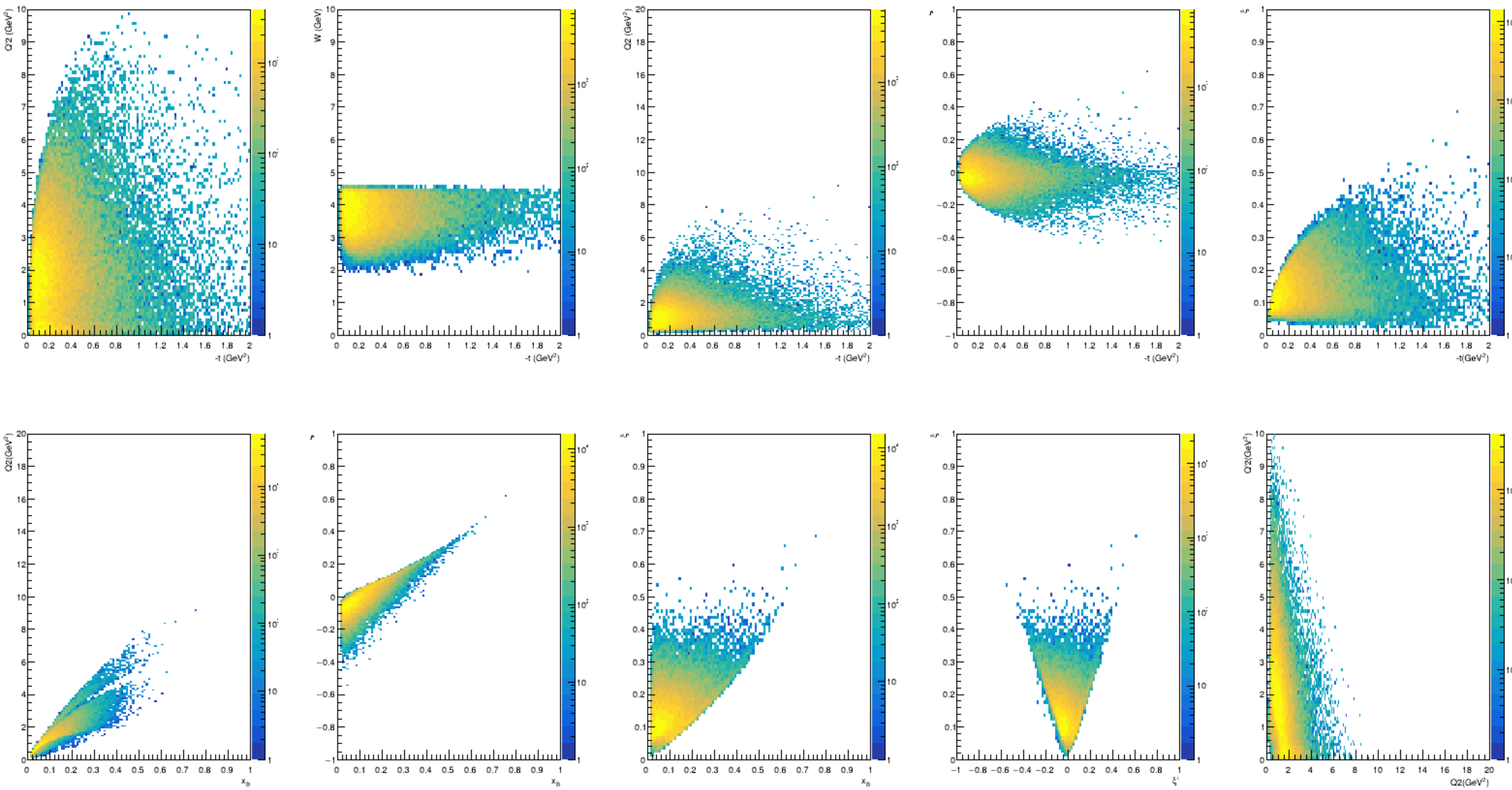

Zhiwen Zhao (GRAPE)

Kinematical coverage 11 GeV

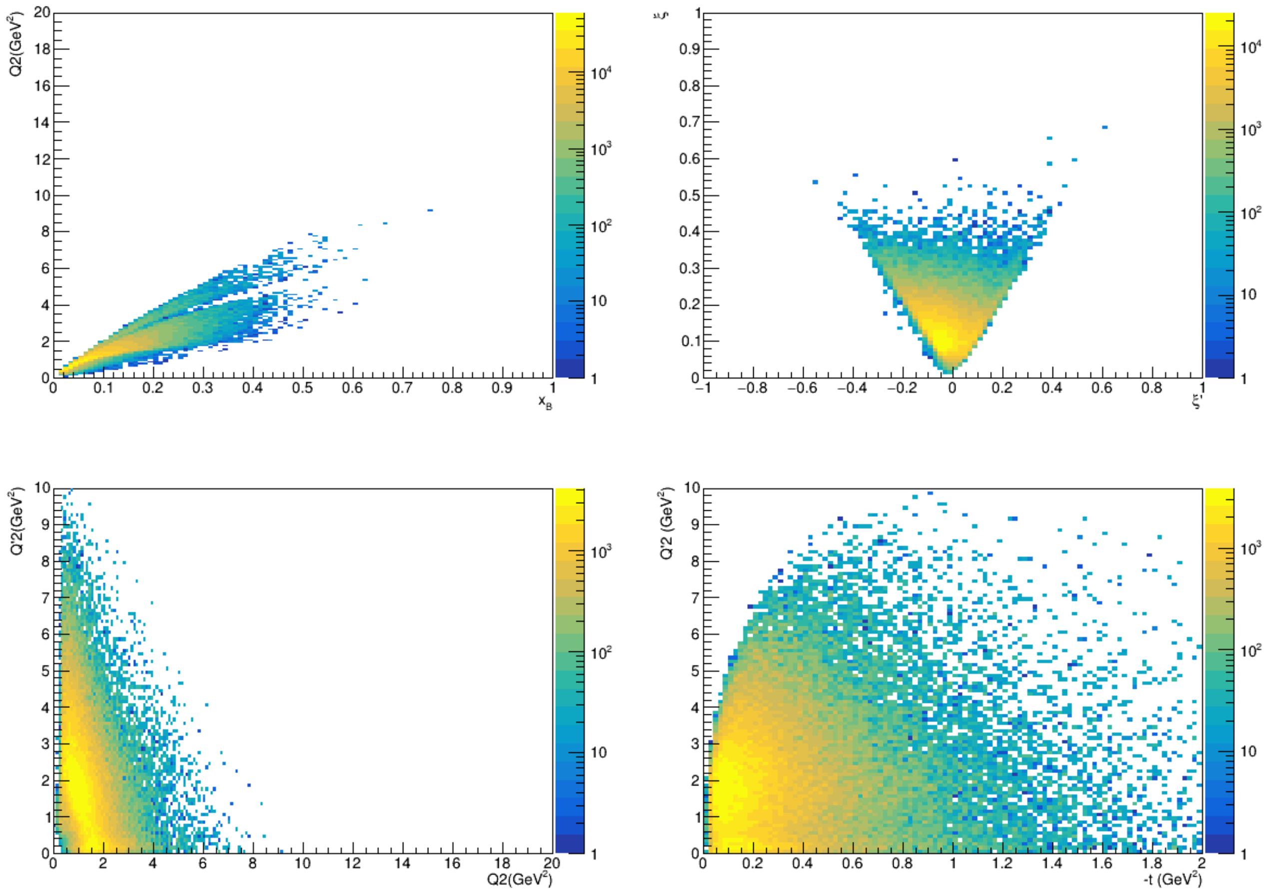

Zhiwen Zhao (GRAPE)

Kinematical coverage 22 GeV

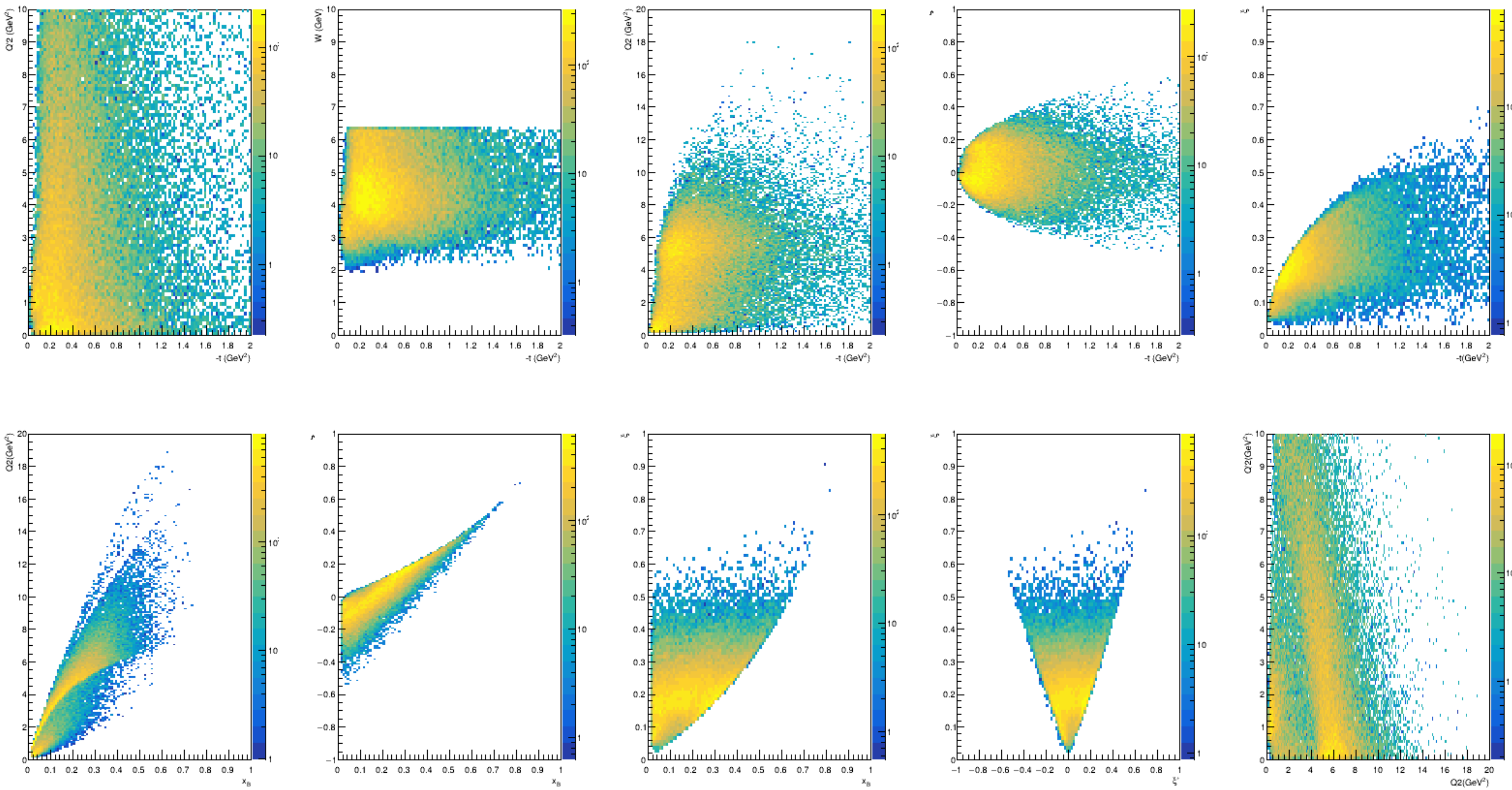

Zhiwen Zhao (GRAPE)

Kinematical coverage 22 GeV

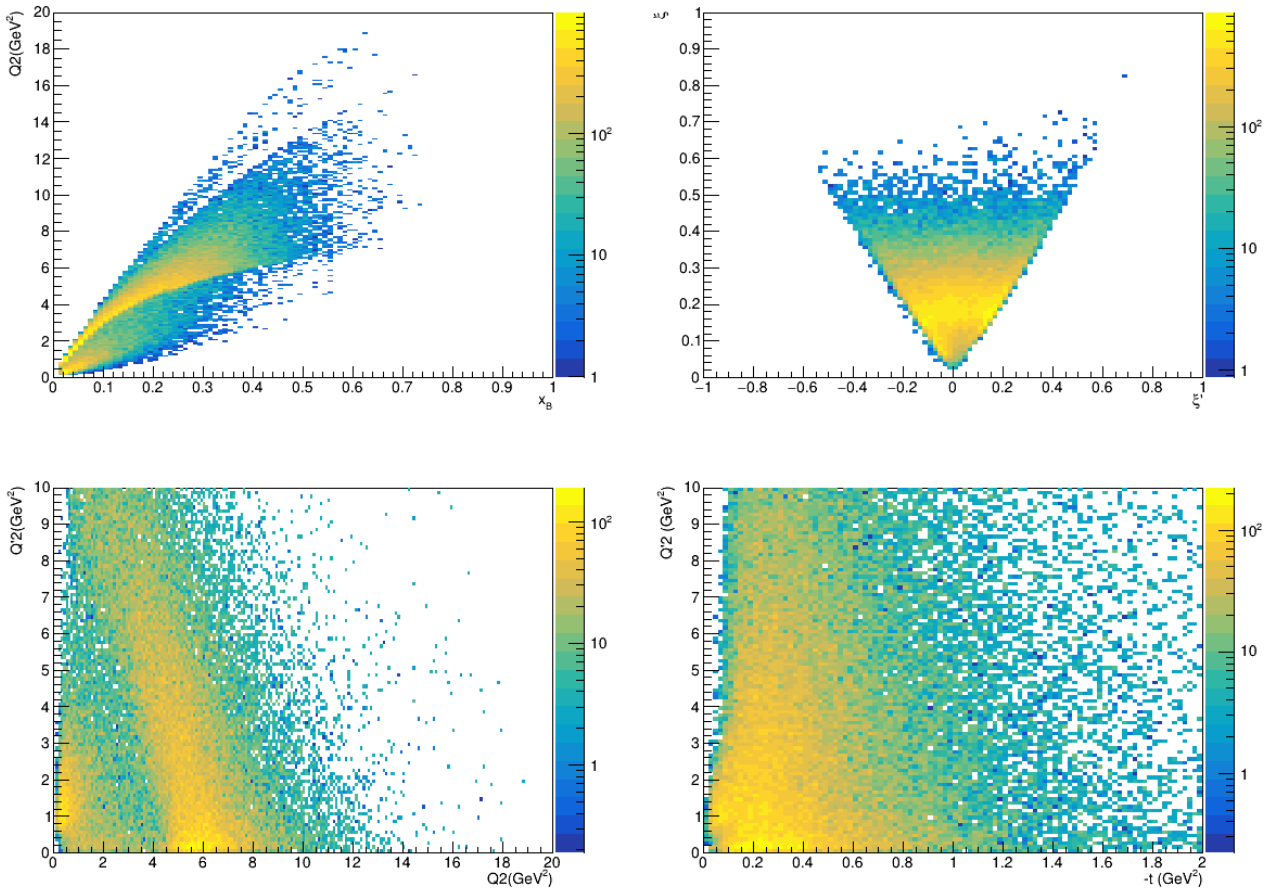

Zhiwen Zhao (GRAPE)

11 GeV vs 22 GeV

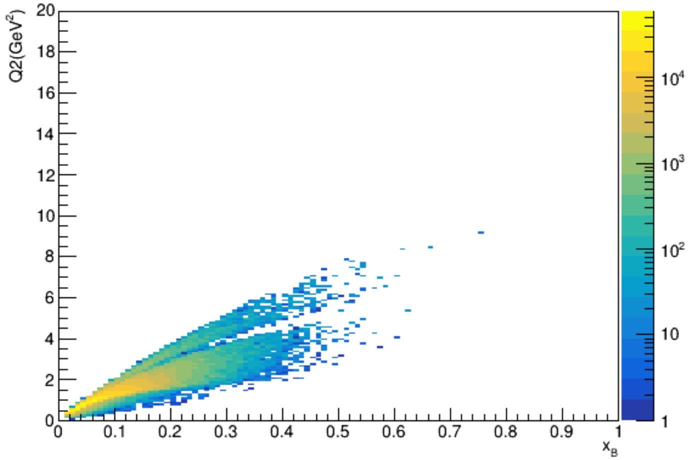

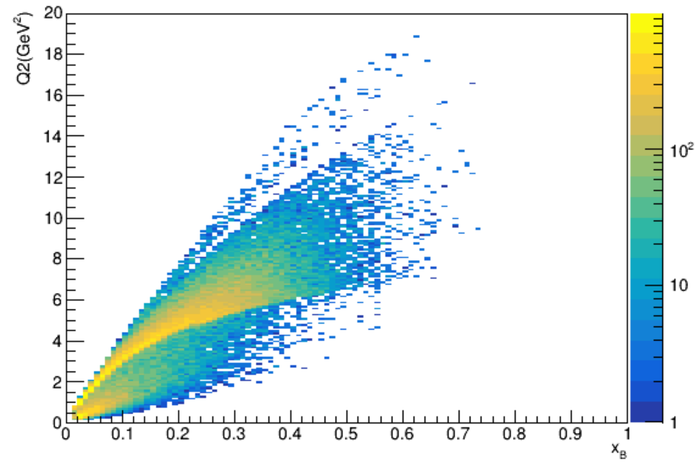

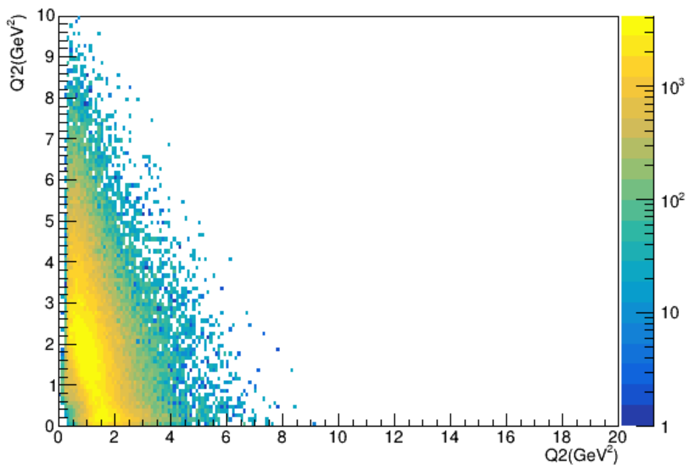

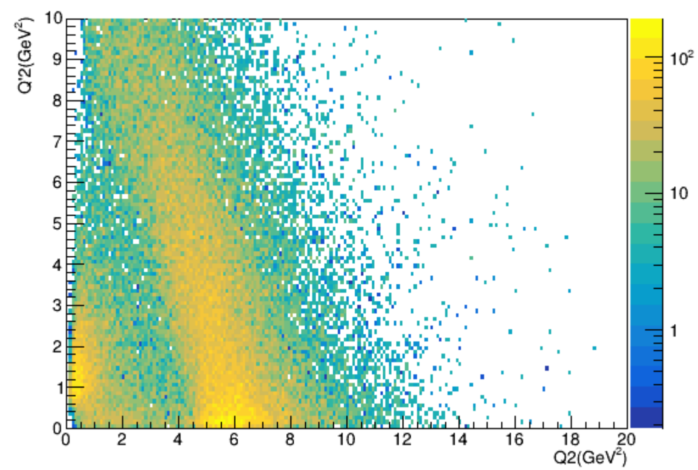

Zhiwen Zhao (GRAPE)

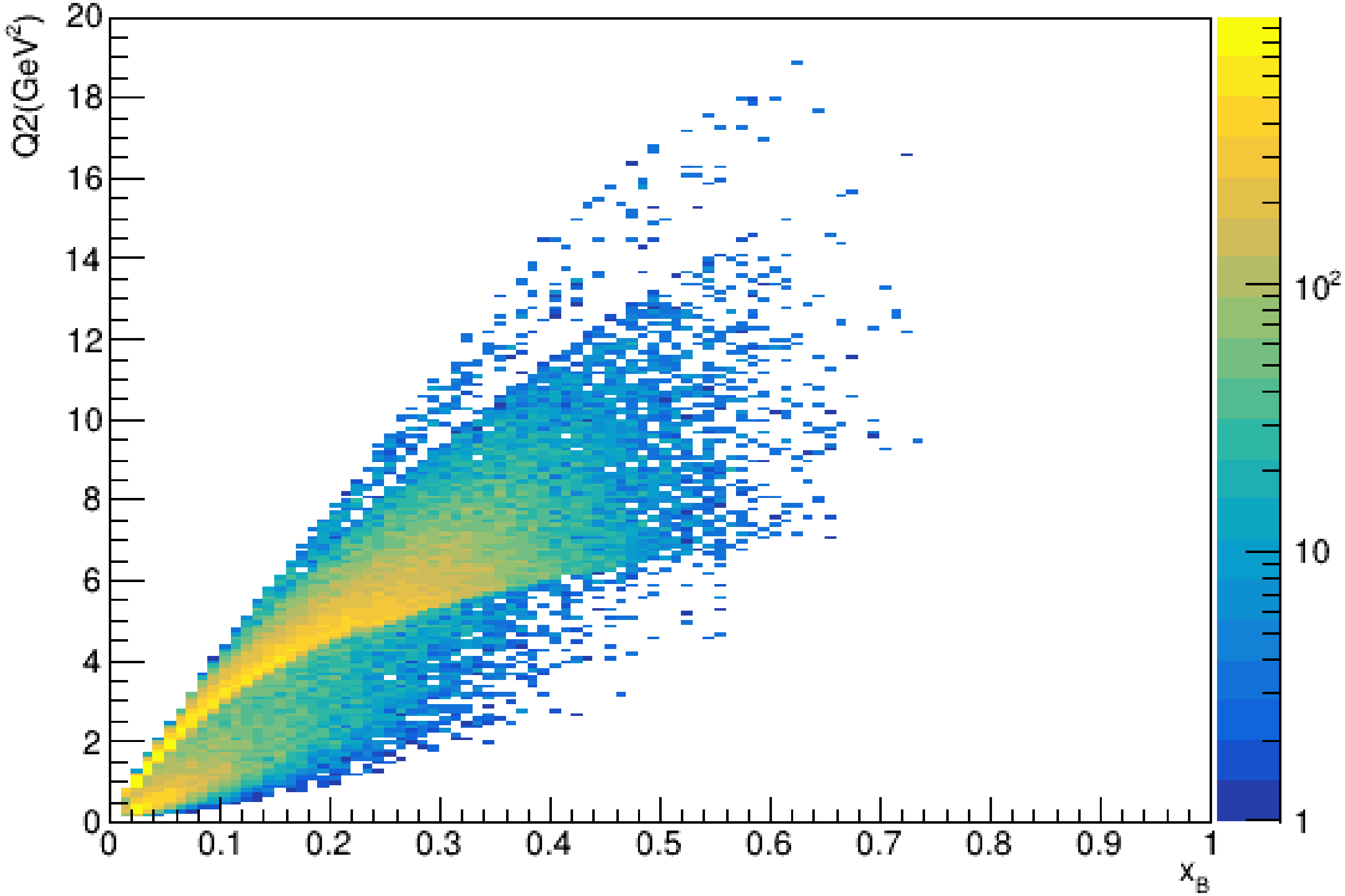

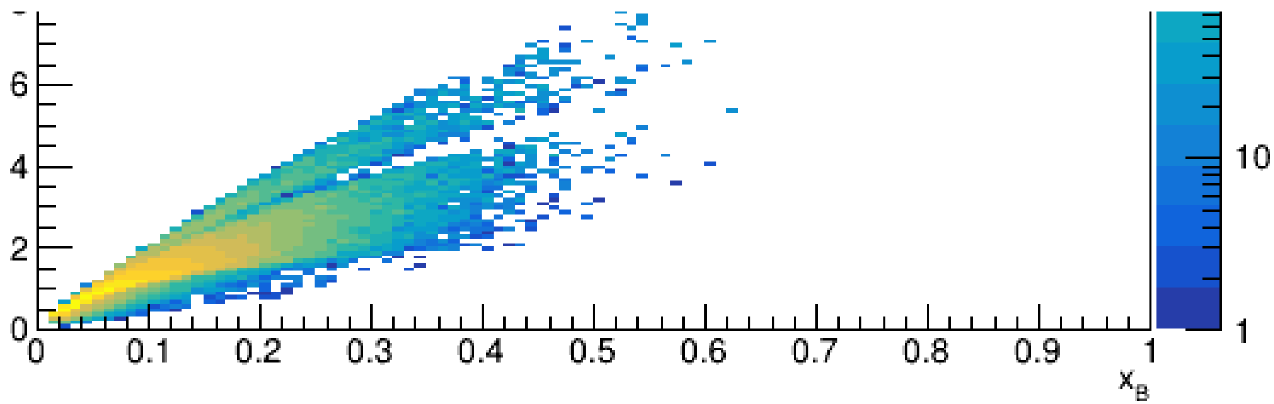

Zhiwen Zhao (GRAPE)

11 GeV vs 22 GeV

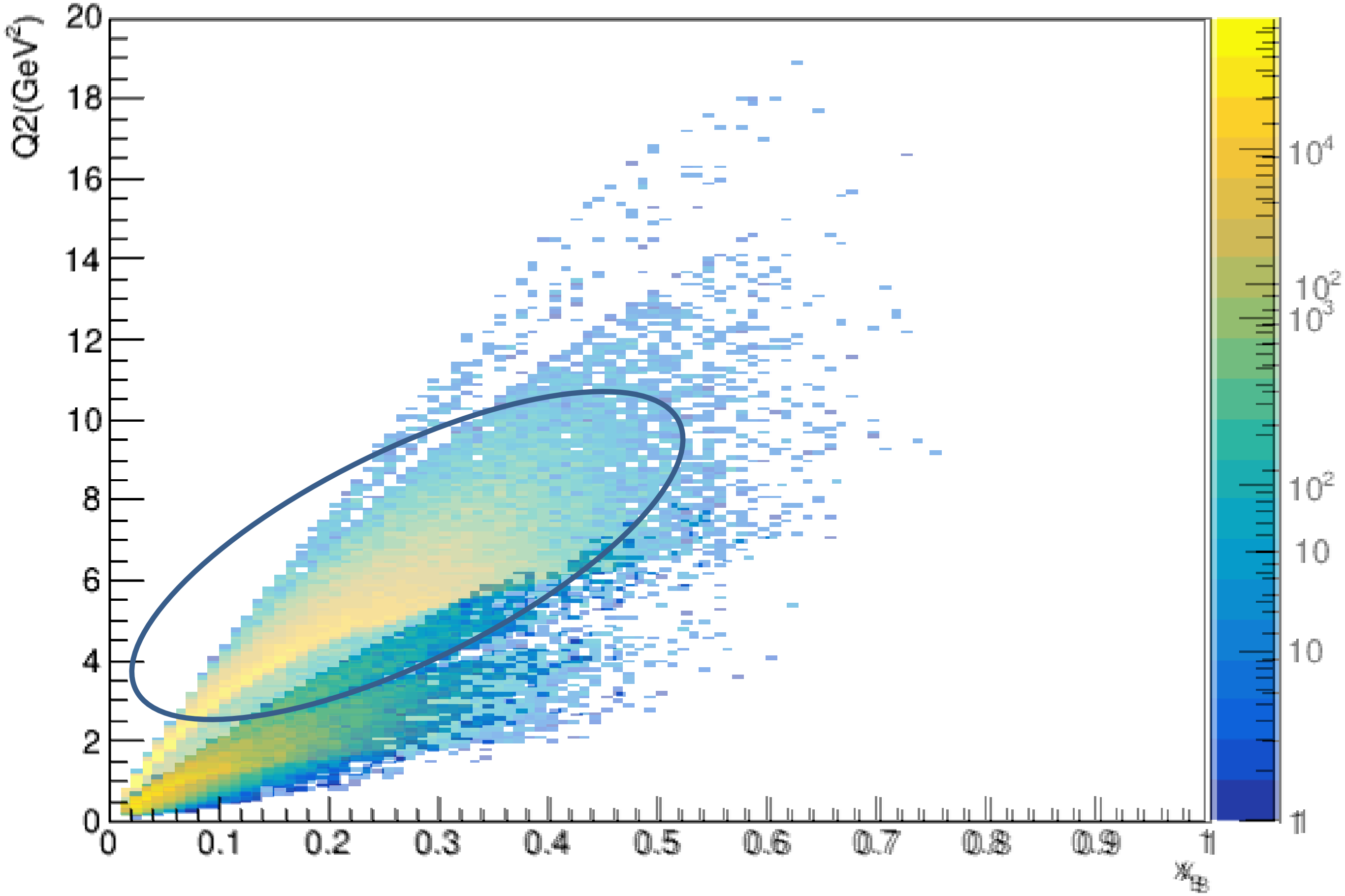

Zhiwen Zhao (GRAPE)

11 GeV vs 22 GeV

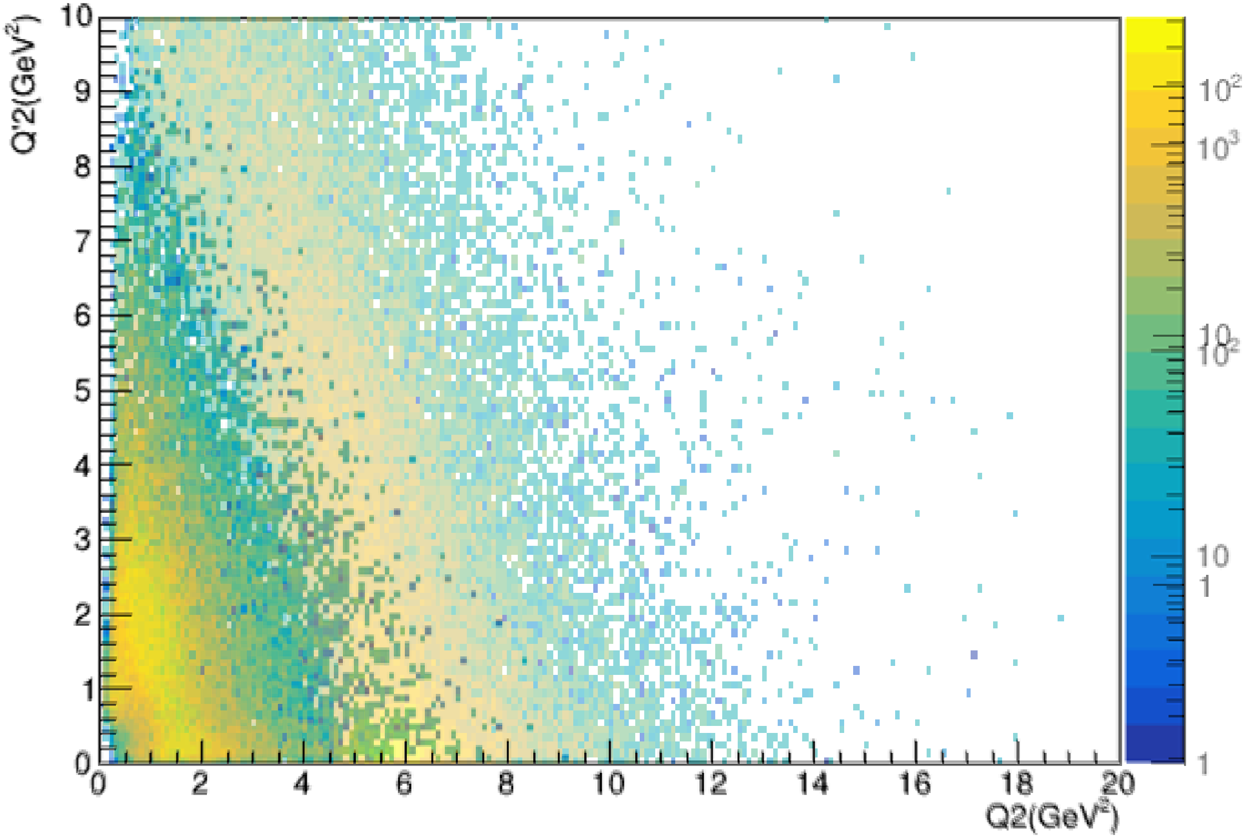

Much better Q2 Q’2 coverage

Want Q2 and Q’2 large enough for factorization

Zhiwen Zhao (GRAPE)

Quick numbers for J/Psi settings

50 days at 10^37

Beam energy	e-mu-mu+	pmu-mu+
11	180156	1.37175e+06
22	51600	2.75867e+06

Cross section about 3 times lower : could run at 10 uA or with 45 cm target

Acceptance better when detecting proton but dominated by low Q2/Q’2

Charged Lepton Flavor Violation ($e^+ \to \mu^+$)

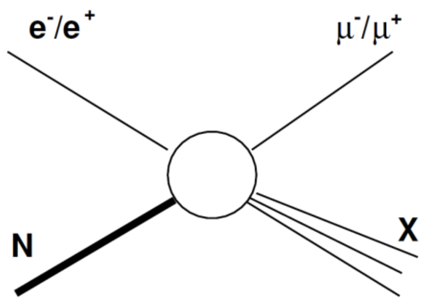

$$e^+ + N \to \mu^+ + X$$

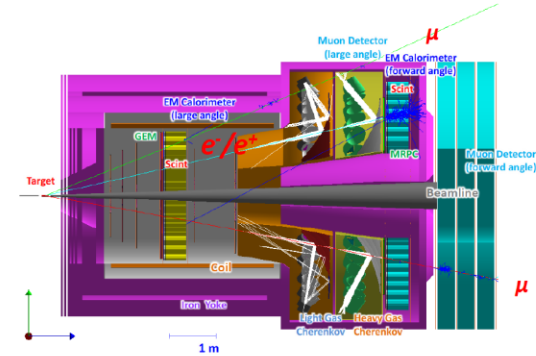

Fig. 3. The SoLID J/Ψ configuration with muon detectors [28]. Other sub-detectors are labeled.

- Low center of mass energy but high luminosity:

$$\sqrt{s} \sim 4.5\ \mathrm{GeV}$$
$$\mathcal{L} \sim 10^{36}\ \text{-}\ 10^{39}\ \mathrm{cm}^{-2}\ \mathrm{s}^{-1}$$

- Detectors should be equipped with muon detectors and a good tracker. Proposed SoLID spectrometer meets these requirements

- High luminosity will allow for substantial improvement over HERA limits on CLFV.

- For $\mathcal{L} \sim 10^{38}\ cm^{-2}s^{-1}$ one can expect two to three orders of magnitude improvement over HERA.

Yulia Furletova
and Sonny Mantry

Charged Lepton Flavor Violation via Leptoquarks

- Convenient to study CLFV in Leptoquark framework which mediates CLFV at tree-level:

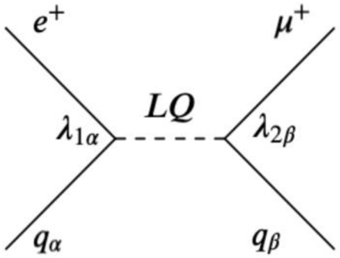

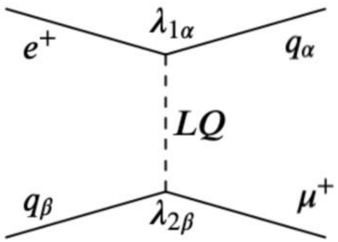

$$\sigma_{F=0}^{e^+p} = \sum_{\alpha,\beta} \frac{s}{32\pi} \left[\frac{\lambda_{1\alpha}\lambda_{2\beta}}{M_{LQ}^2}\right]^2 \int dx \int dy \left\{ x q_\alpha(x, xs) f(y) + x \bar{q}_\beta(x, -u) g(y) \right\}$$

$$\sigma_{|F|=2}^{e^+p} = \sum_{\alpha,\beta} \frac{s}{32\pi} \left[\frac{\lambda_{1\alpha}\lambda_{2\beta}}{M_{LQ}^2}\right]^2 \int dx \int dy \left\{ x \bar{q}_\alpha(x, xs) f(y) + q_\beta(x, -u) g(y) \right\}$$

- 14 LQ states. Positron beam can help disentangle F=0 and |F|=2 LQ states. Polarized beams can help distinguish between left-handed and right-handed LQs.

Type	J	F	Q	ep dominant process	Coupling	Branching ratio β_ℓ
S_0^L	0	2	$-1/3$	$e_L^- u_L \to \ell^- u$	λ_L	1/2
				$\to \nu_\ell d$	$-\lambda_L$	1/2
S_0^R	0	2	$-1/3$	$e_R^- u_R \to \ell^- u$	λ_R	1
$\tilde{S}_0^R$	0	2	$-4/3$	$e_R^- d_R \to \ell^- d$	λ_R	1
S_1^L	0	2	$-1/3$	$e_L^- u_L \to \ell^- u$	$-\lambda_L$	1/2
				$\to \nu_\ell d$	$-\lambda_L$	1/2
			$-4/3$	$e_L^- d_L \to \ell^- d$	$-\sqrt{2}\lambda_L$	1
$V_{1/2}^L$	1	2	$-4/3$	$e_L^- d_R \to \ell^- d$	λ_L	1
$V_{1/2}^R$	1	2	$-1/3$	$e_R^- u_L \to \ell^- u$	λ_R	1
			$-4/3$	$e_R^- d_L \to \ell^- d$	λ_R	1
$\tilde{V}_{1/2}^L$	1	2	$-1/3$	$e_L^- u_R \to \ell^- u$	λ_L	1

Type	J	F	Q	ep dominant process	Coupling	Branching ratio β_ℓ
V_0^L	1	0	$+2/3$	$e_R^+ d_L \to \ell^+ d$	λ_L	1/2
				$\to \bar{\nu}_\ell u$	λ_L	1/2
V_0^R	1	0	$+2/3$	$e_L^+ d_R \to \ell^+ d$	λ_R	1
$\tilde{V}_0^R$	1	0	$+5/3$	$e_L^+ u_R \to \ell^+ u$	λ_R	1
V_1^L	1	0	$+2/3$	$e_R^+ d_L \to \ell^+ d$	$-\lambda_L$	1/2
				$\to \bar{\nu}_\ell u$	λ_L	1/2
			$+5/3$	$e_R^+ u_L \to \ell^+ u$	$\sqrt{2}\lambda_L$	1
$S_{1/2}^L$	0	0	$+5/3$	$e_R^+ u_R \to \ell^+ u$	λ_L	1
$S_{1/2}^R$	0	0	$+2/3$	$e_L^+ d_L \to \ell^+ d$	$-\lambda_R$	1
			$+5/3$	$e_L^+ u_L \to \ell^+ u$	λ_R	1
$\tilde{S}_{1/2}^L$	0	0	$+2/3$	$e_R^+ d_R \to \ell^+ d$	λ_L	1

Crossection proportional to center of mass energy ~ factor 2 at 22 GeV

Yulia Furletova
and Sonny Mantry

SoLIDμ vs μCLAS12

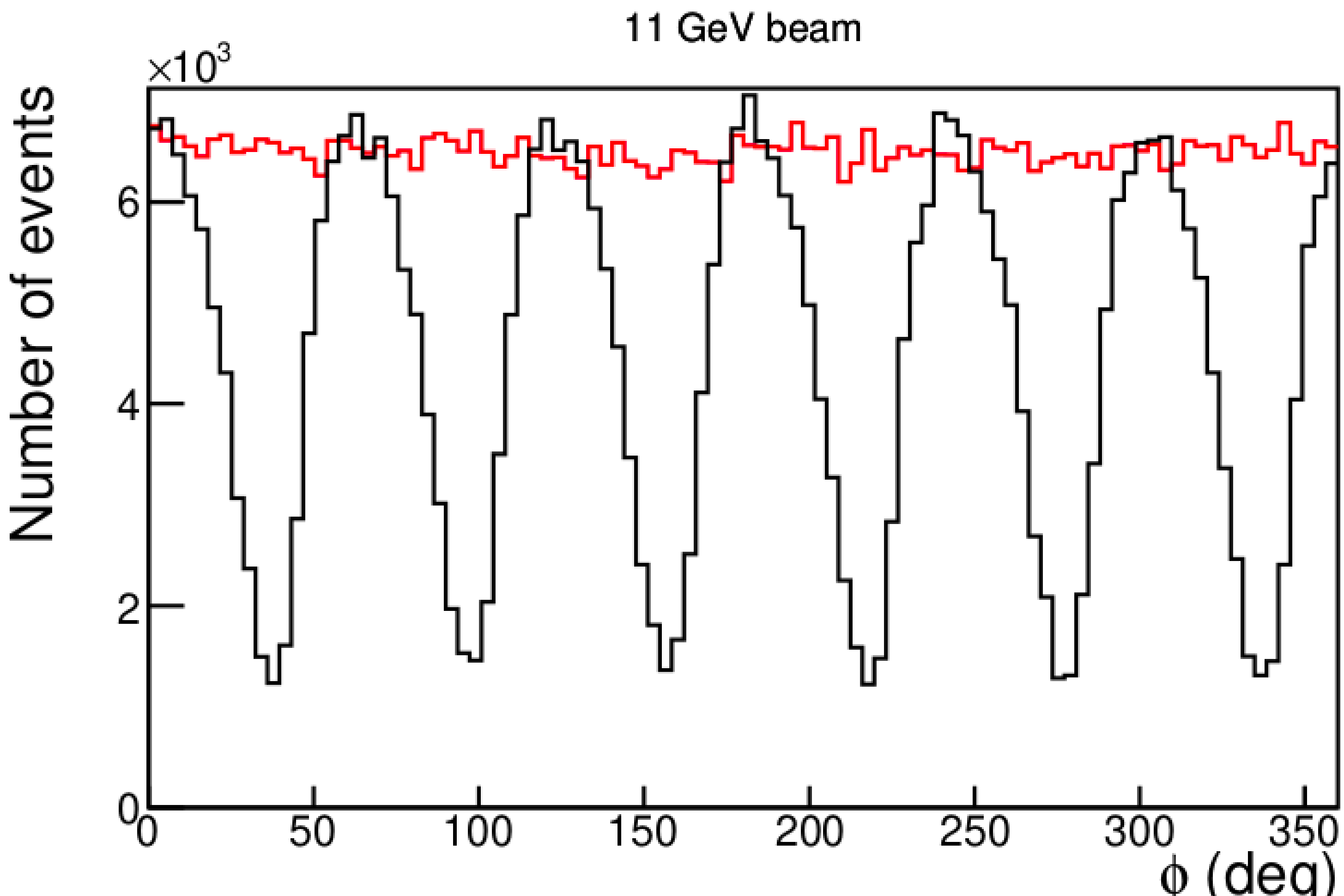

100 days comparison

SoLIDμ vs μCLAS12

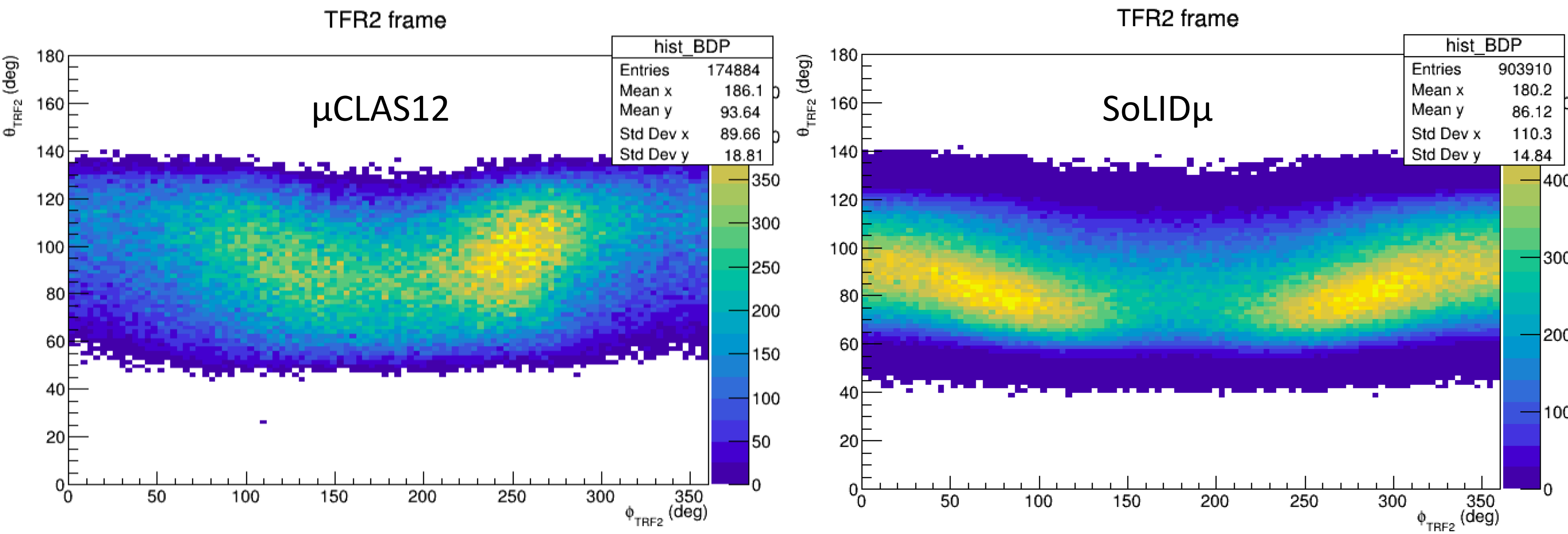

- Angles in the muon center-of-mass frame
- Larger coverage with SoLIDμ

TAC report

1. This proposal will use SoLID with addition of 3-layers of muon detectors, which reuse the iron plates from CLEO (now at JLab) with new tracking detectors and scintillators. Part of the running (10 days calibration, 50 days production) is parasitic to the approved SoLID-J/psi (E12-12-006) experiment and additional 50 days beam time is requested.
2. The proposed measurement, aiming for a first dedicated precision DDVCS measurement, will also enhance the approved SoLID-J/psi and TCS measurements.
3. The J/psi configuration of the SoLID setup has gone through several JLab/DOE reviews and prototype tested with pre-R&D activities. The muon detector is a new design with its performance simulated. A rough estimation of cost was provided.
4. When estimating the additional trigger rate from "di-muon" events (18KHz) it was assumed that the two single rates in 3rd layer are uncorrelated and that a 50 ns time window was used to obtain the accidental coincidence rate. However, there could be single surviving pion/muon events with a correlated additional hit (secondary particle from single pion/muon hitting materials before 3rd layer and then the secondary particle producing a hit in 3rd layer in coincidence with the single pion/muon event). These type of "di-muon" events will not be reduced by the 50 ns window. Is there an

estimate of the rate of these correlated two-hit events that would be included in the "di-muon" trigger rate?

5. To not be overwhelmed by low energy electrons, the J/psi trigger has ECal threshold cuts. The acceptance plots (figures 14-16) seem to not have the low momentum limits corresponding to the ECal threshold cuts. Are the physics projections corresponding to the acceptance of these plots or the acceptance with ECal trigger cuts?

6. The control of systematics of the detector efficiency and acceptance needs more careful study. Simulations alone will not be enough. Calibrations with measurements of specific physics channels may work well for the electron detection, but not clear how well they will work for the muon detector. No clear justifications were given for the "worst case scenario" or the "more reasonable case" (page 37).

Systematics

	Correction/ accuracy	Systematic
Electron efficiency	30%	5%
Acceptance	3%	3%
Polarimetry	1%	1%
Beam charge	3%	3%
Single pion contamination	5%	5
Di-pion contamination	5%	5
Background subtraction	4%	2%

~ 10% systematic on cross section – 5% on assymetries depending on pion asymmetry